Contents lists available at ScienceDirect

Arabian Journal of Chemistry

journal homepage: www.ksu.edu.sa

Enhanced coloration and functionality of wool fabric by Hydroxypropyl-β-cyclodextrin coated magnetic nanoparticles

Xuemei He *, Guangyun Deng, Zhengkang Zhang, Haiyan Mao, Lu Cai

School of Textiles and Clothing, Yancheng Institute of Technology, Yancheng, Jiangsu 224051, China

ARTICLE INFO

Keywords:
Wool
Hydroxypropyl-β-cyclodextrin
Lipoic acid
Magnetic particles
Dyeing

ABSTRACT

The functionality and excellent low temperature dyeability of wool fabrics play a crucial role in expanding their potential applications in the fields of healthcare and technical textiles. The study proposes a highly effective modification method to impart coloration enhancement and functionality for wool fibers using lipoic acid (LA) as a coupling agent to bind hydroxypropyl-β-cyclodextrin (HP-β-CD) capped magnetic nanoparticles (Fe_3O_4). The structure and morphology of the modified wool fabrics (MWF) were characterized by various measure techniques including FT-ATR, FE-SEM/EDS, XRD, X-ray photoelectron spectroscopy (XPS) and thermogravimetric analysis (TG). The results demonstrated the successful immobilization of HP-β-CD capped Fe_3O_4 nanoparticles on the surface of wool fibers through LA. The MWF exhibited enhanced wettability, anti-wrinkle performance, improved UV resistance, effective antioxidation, and good antibacterial effect against Gram-positive (Staphylococcus aureus). These properties were found to be dosage-dependent on LA. In addition, the dyed MWF with Curcumin and Acid red 1 demonstrated higher color strength compared to untreated wool, and the color strength (K/S value) reached to 17.1 and 23.4 respectively when using 4% (o.w.f) dye concentration at 80℃ without any pH adjustment. Furthermore, the dyed MWF with both dyes exhibited the improved rubbing and washing colorfastness. This study presents a potential effective approach for enhancement in the bio-functionality and dyeability of wool fabrics.

1. Introduction

Recently, the utilization of eco-friendly multifunctional textile fibers has shown an upward trend in textile fields due to concerns about ecological and human health safety issues (Adeel et al., 2022; Rehan et al., 2023; Teli & Pandit, 2018). As an important textile raw material, wool is popular with consumers due to its many advantages, such as robust mechanical properties, remarkable moisture transmission, and thermal preservation capability, excellent elasticity (Houshyar et al., 2019; Zhu et al., 2023). However, the hydrophilicity and dyeability of pure wool fabric are not satisfactory, and it lacks multifunctional properties such as antioxidation, antimicrobial activities, anti-crease and anti-felt properties, as well as antistatic properties (Sadeghi-Kiakhani & Safapour, 2015). These limitations restrict its application in the fields of medical textiles, health textiles, and technical textiles (Fazal ur et al., 2022; Hayat et al., 2022; Yan et al., 2022). Furthermore, the conventional wool dyeing conditions with acid dyes require high-temperature boiling and a strongly acidic environment, which easily led to the fiber felting, loss of strength, high energy consumption, and deterioration of water quality (Mia et al., 2021; Wu et al., 2022). The use of natural dyes in wool dyeing is both eco-friendly and beneficial to health due to its nontoxicity, biodegradability, sustainability, anti-oxidation and antibacterial activity, etc., however, it still faces some limitation, such as inadequate dye absorption and suboptimal color-fastness due to its low affinity towards wool fiber. (Bahtiyari & Yılmaz, 2018; Çelik Yılmaz et al., 2023). To enhance dye up-take on wool fiber and impart additional protective function for further application, many methods were applied to wool processes, for example, plasma treatment (Haque & Naebe, 2023), nanoparticle doped, oxidation or reduction, polymer resin deposition (El-Sayed et al., 2022), natural plant extract (Yilmaz, 2020; Yılmaz, 2023), and so on (Banitorfi Hoveizavi & Feiz, 2023; Luo et al., 2023). At present, the incorporating of natural extracts (Azab et al., 2023; Safapour et al., 2024a; Safapour et al., 2024b), biological molecules (Sadeghi-Kiakhani et al., 2022), micro or nano-particles particles into wool textiles is considered to be the most effective and bio-friendly way to improve its dyeing properties and impart functionality (Parveen et al., 2021; Sadeghi-Kiakhani et al., 2021; Safapour et al., 2024a; Shavandi & Ali, 2019; Yılmaz et al., 2020;

* Corresponding author.
E-mail address: hexuemeitry@163.com (X. He).

https://doi.org/10.1016/j.arabjc.2024.105923
Received 12 May 2024; Accepted 21 July 2024
Available online 23 July 2024

Zare, 2023).

Fe_3O_4 magnetic nanoparticles (MNPs) has attracted more and more concern due to their small size, large specific surface area, unique magnetic properties, ease of separation, and antibacterial activity (Niu et al., 2023). Magnetic functional nanomaterials have been widely used in catalysis, biomedicine, magnetic resonance imaging, data storage, adsorption and separation, electrochemical detection, and drug delivery (Aksu Demirezen et al., 2023; Prabhu et al., 2015). However, Fe_3O_4 nanoparticles still possessed some defects such as poor dispersion, susceptibility to agglomeration, and instability (Okasha et al., 2023; Wang et al., 2012). Hydroxypropyl-β-cyclodextrin (HP-β-CD) is a derivative of cyclodextrin, which is a cyclic macromolecule with a hydrophilic exterior and hydrophobic interior, thus having good solubility in water (Corchete et al., 2022; Safapour et al., 2022). The enhancement of dispersion and stability in aqueous solutions for Fe_3O_4 nanoparticles or other nanoparticles has been achieved through the application of hydroxypropyl-β-cyclodextrin (Jiang et al., 2021b; Zhang et al., 2019a; Zhang et al., 2021). For example, Fe_3O_4 nanoparticles were decorated with hydroxypropyl-β-cyclodextrin and polyethylene glycol 400 for the removal of Congo red by Yu et al (Yu et al., 2014). However, the immobilization of Fe_3O_4 nanoparticles on fiber is also an important issue in achieving a surface with multifunctional properties. Taking account of environmental issues, an environmentally acceptable and friendly couple agent is in need without potentially dangerous external chemicals for the Fe_3O_4 nanoparticle immobilization on the fiber surface (Rehan et al., 2023). Alpha-lipoic acid (ALA, 1,2-dithiolane-3-pentanoic acid), as a naturally small biological molecule found in humans and animals, has attracted significant interest for its powerful biological antioxidant activity derived from the disulfide heterocyclic ring in its structure (Theodosis-Nobelos et al., 2021; Wagner et al., 1956; Xu et al., 2020a). It can prevent the damage of free oxygen species to tissue cells and slow down cell aging by directly scavenging free radicals (–OH), reactive oxygen species (ROS), reactive nitrogen species (RNS), singlet oxygen species ($1O_2$), nitric oxide species (NO), etc. (Dolinina et al., 2020; Hwang et al., 2015). Lipoic acid is easily polymerized and transformed into poly-α-lipoic acid at a certain temperature. Lipoic acid and its copolymer have been used in textile fiber as a functional material. For instance, Wu et al. reported using a two-step method to graft polymerized alpha-lipoic acid (ALA) onto silk fibers. Poly-α-lipoic acid (PALA) was formed on the fiber surface through a reduction–oxidation process to improve the electronegativity of the fiber surface for cationic dyeing and impart silk fabrics a significant wrinkle resistance effect (Wu et al., 2022). Huang et al prepared high crease resistance and hydrophilic cotton fabric without strength loss and formaldehyde release, usingα-lipoic acid as an anti-crease agent (Huang et al., 2021). However, these alpha-lipoic acid-modified fabrics had still unsatisfactory bioactivity and low adsorption effect on dyes after poly-α-lipoic acid modification due to the weak binding forces under neutral conditions. Nevertheless, ALA is easily decomposed by photoirradiation and heating resulting in the loss of its physiological activity, which limits its applications in various fields (Ikuta et al., 2014). Therefore, it is also important to keep its activity and stability by modification. Cyclodextrins and its derivatives have been proven to be effective in improving the thermal stability and photostability of LA by encapsulation technique (Celebioglu & Uyar, 2019; Dolinina et al., 2020; Maleki et al., 2022). Furthermore, the solubility and bioavailability of the bioactive compounds can be enhanced by cyclodextrin inclusion complexation. For instance, Ikuta et al. stabilized RALA through complex formation with γ-CD yielding RALA-CD (Ikuta et al., 2014). It is known that wool is a typical keratin-rich fiber material that contains more cysteine residues and disulfide bonds (Zhang et al., 2022a). The cysteine of wool easily occurred self-degradation and produced a thiol group when exposed to moisture and heat, which provides many possibilities for the surface functionalization of wool (Hosseinkhani et al., 2017; Razmkhah et al., 2021). Therefore, based on the aforementioned analysis, HP-β-CD could potentially serve as the stabilizing agent for Fe_3O_4 nanoparticles and LA molecules. Additionally, the latter can effectively immobilize the nanoparticles onto wool fibers through thiol reaction. Importantly, these substances have been demonstrated no harm to human health and the environment (Safapour et al., 2024b). To our knowledge, the incorporation of HP-β-CD, Fe_3O_4 nanoparticles and LA into wool fiber simultaneously have been seldom reported in the literature.

Hence, in this study, hydroxypropyl-β-cyclodextrin and Alpha-lipoic acid can be simultaneously employed as coupling agents and stabilizers of Fe_3O_4 nanoparticles to enhance wool dyeability while imparting bioactivity and functionality. The structure and morphology of modified wool were characterized using various analytical techniques, including Fourier-transform attenuated total reflection infrared spectroscopy (FT-ATR), field emission scanning electron microscopy (FESEM), energy dispersive spectroscopy (EDS), X-ray diffraction (XRD), X-ray photoelectron spectroscopy (XPS), and thermogravimetric analysis (TG). The influence of the LA dosage on the coloration, UV resistant capacity, antimicrobial activities, and anti-crease properties of the wool fibers was evaluated. Furthermore, the dyeing properties of MWF with curcumin and Acid red 1 were investigated under different pH levels, temperatures, dye concentrations, and dyeing time.

2. Experimental

2.1. Experimental materials

Wool knitted plain fabric (100% pure, 90 g/m^2) was obtained from Jiangsu Sunshine Group Co., Ltd., (Shanghai, China). Hydroxypropyl-β-Cyclodextrin (HP-β-CD), iron (III) chloride hexahydrate ($FeCl_3{\cdot}6H_2O$), sodium acetate anhydrous, acetone, ethylene glycol, acetic acid (CH_3COOH), hydrochloric acid, phosphoric acid (H_3PO_4) and boric acid (H_3BO_3), Alpha-lipoic acid (LA) and ethanol were of analytical grade and were purchased from Guoyao Chemical Co. (Shanghai, China). 1,1-Diphenyl-2-picrylhydrazyl Free Radical (DPPH) was purchased from Aladdin in China. Curcumin (98%) was purchased from Xi 'a Ruidi Biological Technology Co., LTD. C.I. Acid red 1 was supplied by Ruixiang Dye Co. (Tianjin, China).

2.2. Preparation of HP-β-CD/Fe_3O_4 /LA solution

The magnetic Fe_3O_4 solution was prepared following a previously reported method with minor adjustments (He et al., 2022). In brief, 2.7 g of $FeCl_3{\cdot}6H_2O$ was dissolved in 80 mL of glycol, the resulting solution was stirred magnetically until it became clarity. Subsequently, 7.2 g of sodium acetate anhydrous was added under stirring until the mixture transformed into a viscous and homogeneous brown-yellow nano-Fe_3O_4 solution. Secondly, 0.2 g of LA dissolved in 20mL absolute ethanol was gradually added into 80mLof 2.5 % (m/v) hydroxypropyl cyclodextrin aqueous solution under continuous stirring for 60min until the hydroxypropyl cyclodextrin/alpha-lipoic acid (HP-β-CD/LA) mixed solution formed. Finally, adding nano Fe_3O_4 solution into the hydroxypropyl cyclodextrin/alpha-lipoic acid (HP-β-CD/LA) solution, keeping stirring for 2h until transparent wine red obtained, thus, the HP-β-CD/Fe_3O_4/LA solution was obtained.

2.3. Preparation of modified wool fabrics

The modification of wool fabrics was conducted in the sealed and conical flasks by using a constant-temperature oscillated dyeing machine. Firstly, the untreated wool samples were scoured with distilled water for 20 min in a bath comprising 2 g/L nonionic detergent with a liquid-to-fabric ratio of 1:50 at 80 °C. Then the samples were rinsed with distilled water and kept to dry at room temperature (Razmkhah et al., 2021). Secondly, the scoured wool fabrics (10×10 cm^2) were immersed in the HP-β-CD/Fe_3O_4 solution and HP-β-CD/Fe_3O_4/LA solution respectively, keeping a constant temperature of 50℃ for 1h under oscillation. Finally, the modified wool fabrics were washed with

deionized water, dried in the oven at 50℃, pressed by using a heat press at 100 °C for 2 min in sequence. Thus, the modified wool fabrics were obtained and respectively denoted as HP-β-CD/Fe_3O_4@WF and HP-β-CD/Fe_3O_4/LA@WF. In addition, according to the 0g, 0.1 g, 0.2 g, 0.3 g, and 0.4 g of LA dosage, the HP-β-CD/Fe_3O_4/LA solution-modified wool fabrics were denoted MWF-LA_0, MWF-$LA_{0.1}$, MWF-$LA_{0.2}$, MWF-$LA_{0.3}$, MWF-$LA_{0.4}$. The corresponding untreated wool fabric is labeled as UWF.

2.4. Dyeing of wool fabrics

Dyeing of the wool before and after modification was completed under different dyeing conditions in a WHY-2 constant temperature shock dyeing machine (Changzhou, Jiangsu Huanyu Scientific Instrument Factory, China). The dyeing process proceeded as follows: The dye concentration was 4% (o.w.f) based on the weight of the fiber, and the liquor ratio was maintained at 100:1. The temperature for dyeing was set at 60 °C with a hold time of 60 min without adjusting the pH of dyebath. After dyeing, the fabrics were rinsed with tap water and air-dried.

2.5. Color parameters and UV resistant test

Color parameters of dyed wool fabrics (Color strength (K/S) &CIE L*, a*, b* values) were recorded on Data color 7000A spectrophotometer (Data color International Ltd, UK). The color strength (K/S value), the lightness (L*), red or greenness (a*), blue or yellowness (b*), and chroma or color saturation (c*) were evaluated under illuminant D65 (He et al., 2024). The K/S were measured for Curcumin and Acid red 1 at maximum wavelength 420nm and 540nm, respectively. Wool samples were put into the YG(B)912E textile UV-protection tester to test the UV resistance.

2.6. Measurement of antioxidation and antibacterial activities

The DPPH assay evaluated the antioxidant activity of wool samples by mixing 2.0 mL of a 0.01 mg/mL ethanol solution with 2.0 mL of 0.1 mM DPPH. After 30 min incubation, absorbance was measured at 517 nm, using absolute ethanol as blank and DPPH without wool samples as control. Antioxidant activity was calculated by equation (1). Modified wool fabrics were tested for antibacterial activity against S. aureus and E. coli using the agar plate method (Dai et al., 2023). Wool fabric pieces were inoculated with bacteria, vortexed, diluted, and cultured on LB agar plates for 18 h at 37°C. Use equation (2) to calculate the bacteria inhibitive rate based on recorded colony count.

$$Antioxidantactivity(\%) = [1 - (As - Ab)/Ac] \times 100 \quad (1)$$

where As is the absorbance of the sample at 517 nm, Ab, and Ac is the absorbance of the blank group and control group at 517 nm, respectively.

$$R = \frac{A_0 - A}{A_0} \times 100\% \quad (2)$$

where R represents the antibacterial efficiency, A_0 represents the number of colonies on the LB agar plate of wool and A represents the number of colonies on the LB agar plate of modified wool.

2.7. Mechanical properties and alkali solubility

The tensile strength of the untreated and modified wool fabrics were recorded with a gauge length of 100 mm and a strain rate of 10mm/min using an electromechanical universal testing machine (CMT4304, MTS SYSTEMS CO, LTD, China). The bursting strength of wool fabrics was measured in accordance with GB/T19976-2005 using the fixed steel ball method on a YG (B) 026E electronic fabric strengthening machine (Wenzhou Darong Textile Instrument Co., LTD).

2.8. Characterization

FTIR-ATR transmission spectra of Untreated wool and modified wool were recorded using a Fourier Transform Infrared spectrometer (Thermo Nicolet 6700, USA) by the KBr pressed-disk method in a spectral range of 4000–400 cm^{-1}. The SEM images and EDS of wool fabrics were taken using Field-emission scanning electron microscopy (Nova NanoSEM 450, SEM). The XPS spectra (ESCALAB250Xi Thermo Fisher Scientific instrument, USA) were used to test the chemical component of wool with the Al Kα X-ray source at a power of 25 W. TG and DTG curves of wool fabrics sample was analyzed using a thermogravimetric analyzer (Type STA-449C; NETZSCH Instrument Co. Ltd.; Germany) in N_2 atmosphere. The temperature ranged from 20 to 700 °C at a scanning rate of 10 °C min^{-1}. The X-ray Diffraction (XRD) curves of wool fabrics were determined by X'Pert^{3}Powder diffractometer (Netherlands PANalytical) with Cu Kα radiation in a range (2θ) between 5 and 60°. The crystallization index (CI) of wool fibers was calculated using the Eq. (3) (Wang et al., 2023b).

$$CI(\%) = 100(I_I - I_{II})/I_I \quad (3)$$

where I_I is the maximum intensity around $2\theta = 9^\circ$ and I_{II} is the minimum intensity near $2\theta = 14^\circ$.

2.9. Fastness properties

The washing, and rubbing fastness of dyed wool fabrics were tested according to ISO 105-C06, and ISO 105-X12, respectively.

3. Results and discussion

3.1. Preparation and structure characterization of modified wool fabrics

The modification of wool fiber was carried out by in-situ deposition method attaching organic and inorganic molecules onto its surface, owing to the presence of various polar groups such as amine, thiol, and carboxyl groups (Hosseinkhani et al., 2017). Initially, Fe_3O_4 nanoparticles were wrapped with HP-β-CD to prevent aggregation. Subsequently, lipoic acid was employed as a coupling agent to attach the HP-β-CD capped Fe_3O_4 nanoparticles onto the surface of wool fiber. This connection allows the HP-β-CD capped magnetic nanoparticles to be effectively fixed to the wool fiber by S-S bond. Furthermore, the formed poly-α-lipoic acid (PALA) molecular chain under hot pressing also can facilitate the efficient reconstruction of disulfide crosslinking with the free sulfhydryl groups on wool molecular chains (Zhu et al., 2023). The preparation mechanism of HP-β-CD/Fe_3O_4 /LA modified wool fabrics was depicted in Fig. 1a.

The chemical structure of different wool fibers was analyzed using FTIR-ATR in Fig. 1b. The infrared spectra of the three types of wool fibers exhibit a high degree of similarity overall. The spectra exhibited absorption bands in the range of 3291∼3370 cm^{-1}, which were attributed to the N-H stretching vibration peak and O-H stretching vibration peak. The characteristic bands at 1643 cm^{-1} (amide I), 1517 cm^{-1} (amide II), and 1240 cm^{-1} (amide III) were attributed to the presence of amide bonds (CONH) in untreated wool fabrics. The band of the disulfide bonds was found to be located at 1037cm^{-1}(Gu et al., 2021). The appeared peak at 2934 cm^{-1} was attributed to the C-H stretching on the spectra of HP-β-CD/Fe_3O_4@WF. Compared with the untreated wool fabric, the absorption peak of amide II at 1517 cm^{-1} was broadened and shifted to 1533 cm^{-1}. A strong peak at 950-1100cm^{-1} and a weak band at 500- 950cm^{-1} were due to the aromatic ring C–H deformation and the aromatic substituents (Gu et al., 2021). The characteristic stretching peak of Fe-O is around 695cm^{-1}, confirming the formation of the hydrogen bond between HP-β-CD capped Fe_3O_4 nanoparticle and wool main chain molecular. The characteristic peak of HP-β-CD/Fe_3O_4/

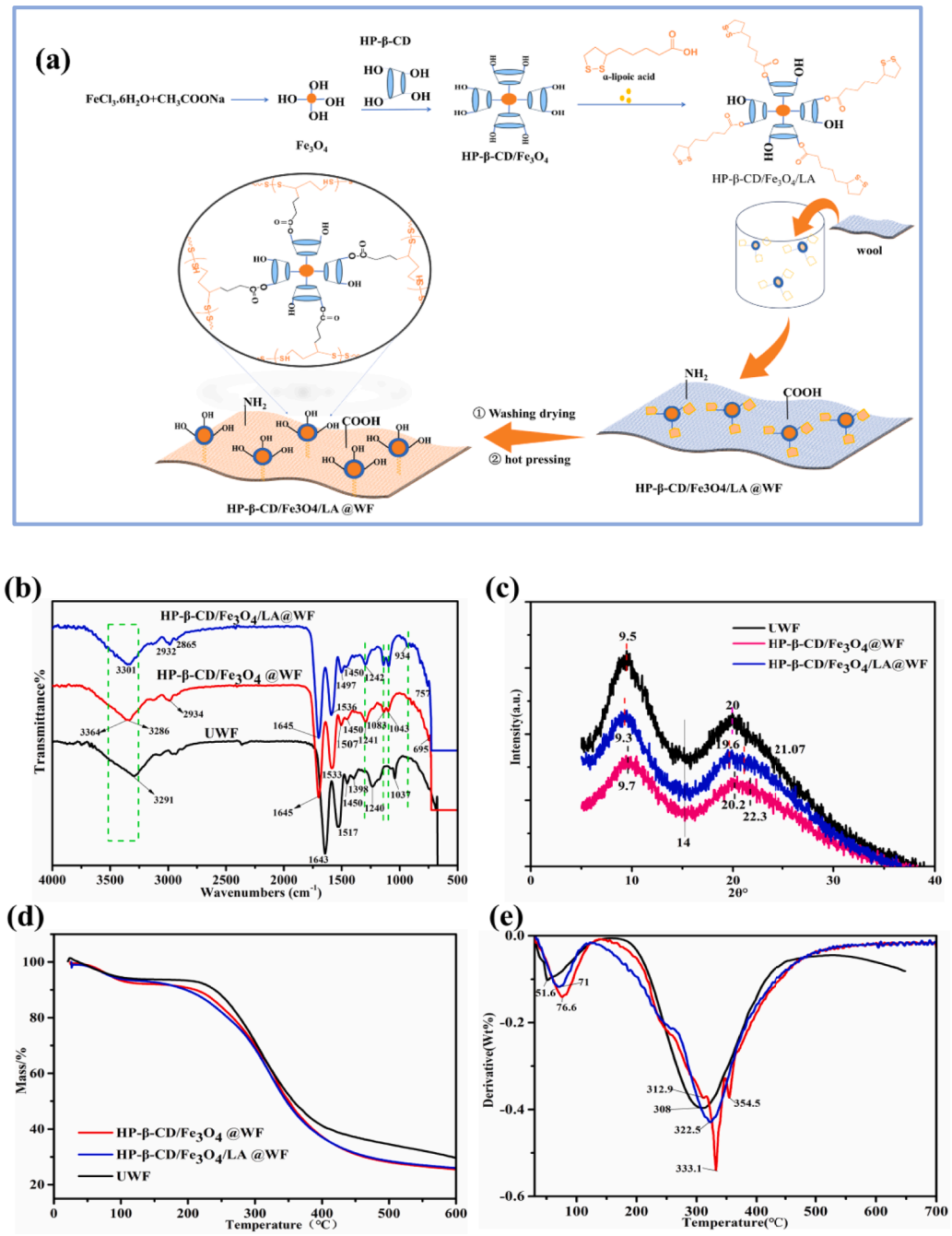

Fig. 1. Preparation mechanism and structure characterization of HP-β-CD/Fe_3O_4/ LA@WF: (a) Preparation mechanism, (b) FTIR-ATR, (c) XRD patterns, (d)TG and (e) DTG curves.

LA@WF the was similar to that of the HP-β-CD/Fe_3O_4@WF. On the spectrum of HP-β-CD/Fe_3O_4/LA@WF, two weak characteristic signals emerged at 1043 cm^{-1} and 984 cm^{-1}, which are related to the S–O and C=S stretching vibration of cystine oxidation products (Afsharipour et al., 2021; Wang et al., 2023b; Zhang et al., 2022a). The spectrum of HP-β-CD/Fe_3O_4/LA@WF exhibited adsorption peaks at 2932 and 2865 cm^{-1}, which were attributed to the asymmetric and symmetric stretching of C-H bonds in HP-β-CD and ALA, respectively. Furthermore, the appeared peak at 934cm^{-1} also indicates the presence and expansion of S-S in modified wool fabrics. The results demonstrate the successful anchoring of HP-β-CD capped Fe_3O_4 particles onto wool fabric surface through lipoic acid.

The structure of wool fabrics was further investigated through XRD analyses in Fig. 1c. In general, an increase in the α-helical structure enhances crystallinity, while an increase in β-sheet content leads to a decrease in crystallinity. The diffraction pattern in Fig. 1c reveals characteristic peaks of wool fiber at 9-10° and 15-31°, which can be attributed to the α-helical and β-sheet structures of wool fibers respectively. Additionally, a peak is observed at 2θ = 14° due to the amorphous nature of the fibers (Zhang et al., 2022a). Hence, for the untreated wool fiber, two distinct peaks at 9.5°and 20°are attributed to the α-helix structure and β-sheet structure, respectively (Jiang et al., 2021a). However, XRD analysis of modified wool fabrics with HP-β-CD/Fe_3O_4 and HP-β-CD/Fe_3O_4/LA reveals a reduction in the intensity of some diffraction peaks, indicating a decrease in the crystallinity of the wool fibers. The peak intensity of HP-β-CD/Fe_3O_4 @WF and HP-β-CD/Fe_3O_4/LA@WF weaken at 2θ=9.7°and 9.3°,respectively, in comparison with UWF, which indicated the decreased tendency of the α-helix structure.

Further, the crystallization index (CI) of wool fibers was calculated using Eq. (3). The crystallization index for UWF, HP-β-CD/Fe_3O_4 @WF, and HP-β-CD/Fe_3O_4/LA@WF was 32.5%, 25.2%, 29.7%. The crystallinity exhibited a decrease due to the incorporation of LA coupling on wool fiber, which disrupts the hydrogen bond or amide group between the fibers (Wang et al., 2023b). As Fig. 1c illustrates, there is a new peak at $2\theta = 22.3^\circ$ and 21.7° on HP-β-CD/Fe_3O_4 @WF and HP-β-CD/Fe_3O_4/LA @WF, respectively, which are attributed to the presence of Fe_3O_4 nanoparticles. The results demonstrated that HP-β-CD capped Fe_3O_4 can be immobilized onto the surface of wool fibers through thiol groups of LA, while the resulting Poly LA can also penetrate into the porous structure of the fibers via Van der Waals forces and hydrogen bonds, leading to disruption of polypeptide chains and inner fiber structure (Teli & Pandit, 2017; Zhang et al., 2019b). The decrease in the crystallization index observed after modification can be attributed to the amorphous nature of the disulfide polymer (Park & Lee, 2013). In all, the increase of amorphous area after modification was favorable to the uptake of dye.

The thermal stability of untreated and modified wool was analyzed using Thermogravimetric analysis (TGA) and its derivative curves (DTG), as depicted in Fig. 1d and 1e. The TGA curves of wool fibers treated in different ways showed similar trends in the main weight loss zones. As shown in Fig. 1d, the occurred initial mass loss for untreated wool, HP-β-CD/Fe_3O_4@WF and HP-β-CD/Fe_3O_4/LA@WF before 150°C was 7.7%,7.3% and 5.6%, respectively. It was due to the evaporation of physical or chemical binding water inside the wool fabric (Rama Rao & Gupta, 1992). The weight loss interval of the second stage primarily occurred within the temperature range of 200℃ to 400℃. The weight reduction percentages were notably high, reaching 53.1%, 59.4%, and 57.2% for untreated wool, HP-β-CD/Fe_3O_4@WF, and HP-β-CD/Fe_3O_4/LA@WF respectively. During this stage, the weight of the wool fabric decreases rapidly due to both the decomposition of polypeptide chains in the wool fiber and the rupture of disulfide bonds (Cai et al., 2023; Singh et al., 2023). At 600℃, residual carbonization of untreated wool, HP-β-CD/Fe_3O_4 @WF and HP-β-CD/Fe_3O_4/LA@WF is 29.5%, 25.2% and 26%, respectively. The initial thermal decomposition temperatures for raw wool fabric, HP-β-CD/Fe_3O_4@WF, and HP-β-CD/Fe_3O_4/LA@WF were approximately 51.6℃, 71℃, and 76.6℃ respectively, as depicted in Fig. 1e. In the second stage, Tmax (the temperature of maximum weight loss) for UNWF, HP-β-CD/Fe_3O_4@WF, and HP-β-CD /Fe_3O_4/LA@WF were found to be 308℃, 333.1℃, and 322.5℃ respectively. These results indicate that the incorporation of Fe_3O_4 nanoparticles with enhanced stabilization contributes to improved thermal stability. However, the bad instability of LA caused the Tmax of HP-β-CD/Fe_3O_4/LA @WF to be lower than that of HP-β-CD /Fe_3O_4@WF (Racz et al., 2013). In summary, the modification treatment has negligible impact on its thermal stability.

Fig. 2a–f indicates FE-SEM images of the untreated wool and modified wool samples in various magnifications (X5000, X20000). The untreated wool surface in Fig. 2a and 2d exhibits a distinct smooth scale layer structure, devoid of any nanoparticles on or within the fabric, while some nanoparticles can be observed both on the surface of HP-β-CD/Fe_3O_4 @WF and HP-β-CD/Fe_3O_4 /LA@WF in Fig. 2b and 2c, indicating the presence of Fe_3O_4 nanoparticles. The polymer-wrapped nanoparticles are loaded uniformly on the wool surface with nano-spherical shapes in Fig. 2e and 2f. After the introduction of lipoic acid, HP-β-CD capped Fe_3O_4 nanoparticles were firmly anchored to the wool fabric, thereby enhancing its surface area and facilitating efficient adsorption of dye molecules. Additionally, Fig. 2g and 2 h depict mapping analysis results illustrating the distribution and approximate quantities of modified wool fabric as detected by EDS. The presence of C, N, S, O, and Fe elements was detected in both HP-β-CD/Fe_3O_4@WF and HP-β-CD/Fe_3O_4/LA@WF. The Fe content was found to be 4.9 % in the HP-β-CD/Fe_3O_4@WF and 11.1 % in the HP-β-CD/Fe_3O_4/LA@WF. Meanwhile, the distribution of Fe_3O_4 nanoparticles throughout both modified wool fabrics is uniform. The ranking of sulfur content was as follows: HP-β-CD/Fe_3O_4/LA@WF > HP-β-CD/Fe_3O_4@WF > Untreated WF, indicating a higher concentration of S in the HP-β-CD/Fe_3O_4/LA@WF sample. The sulfur content of HP-β-CD/Fe_3O_4/LA@WF reached 2.08 %. The results demonstrated the successful bonding of HP-β-CD coated magnetic nanoparticles to wool fibers through disulfide of lipoic acid, as confirmed by FE-SEM, mapping, and EDS analysis. This modification effectively introduced more active groups on the surface of wool fibers, thereby enhancing the dyeing properties and fastness of the dyed samples (Razmkhah et al., 2021).

The chemical elemental compositions of wool fabrics were further determined through XPS analysis. According to the XPS spectra in Fig. 3a, distinct peaks are observed at 285 eV (C 1s), 400 eV (N 1s), 532 eV (O 1s), and 164 eV (S2p) on various wool fabrics. The results were consistent with the reported literature (Zhang et al., 2019a). The untreated wool fabrics primarily consisted of carbon, oxygen, nitrogen, and sulfur; however, the XPS spectra presented in Fig. 3a revealed the presence of iron atoms in HP-β-CD/Fe_3O_4@WF and HP-β-CD/Fe_3O_4/LA@WF. A significant discrepancy was observed in the S2p XPS spectrum among UWF, HP-β-CD/Fe_3O_4@WF, and HP-β-CD /Fe_3O_4/LA@WF in Fig. 3b. The S2p XPS spectrum of UWF exhibited two peaks corresponding to S(II) (−S-S-) and S(IV) (C–SO2–C), located at approximately 164eV and 168eV, respectively (Zhang et al., 2022b). The peak of S2p1/2 is divided into two peaks two features at 163.6 and 164.96 eV, due to C–S–C and C–S–S–C disulfide groups (Li et al., 2022). The presence of a prominent peak at a high binding energy (168.2 eV) suggests that a minor portion of the cystine underwent oxidation during hot pressing (Jiang et al., 2021a; Zhang et al., 2019b). The higher S-S content in HP-β-CD/Fe_3O_4/LA@WF in Fig. 3b is attributed to the presence of S-containing dithiolane within LA. The C1s XPS spectrum of UWF is divided into three peaks in Fig. 3 c, which are 284.5 eV (C-C and C–H, mainly derived from fiber surface peptide chain molecules, 285.4 eV (C–O and C–N), 288.2 eV (O-C-O and −C=O), which is consistent with the reported literature (Ward et al., 1993). The binding energies of the C-O bonds (286.3 eV) and C–C/C-H bonds (284.8 eV) in the HP-β-CD/Fe_3O_4/LA@WF exhibited a slight increase compared to 285.5 and 284.7 eV in HP-β-CD/Fe_3O_4@WF, potentially attributed to the coupling interactions from LA. Compared with the C1s spectrum of the untreated wool (Fig. 3c), the presence of HP-β-CD in HP-β-CD/Fe_3O_4@WF led to an increase in the content of C-C and C-H bonds, resulting in a higher concentration of carbon elements on the surface of wool fibers. The area of C-O, C–S of HP-β-CD /Fe_3O_4/LA@WF was found to be greater than that in UWF and HP-β-CD /Fe_3O_4@WF, suggesting that the formation of disulfide bond between wool fibers in HP-β-CD /Fe_3O_4/LA@WF (Zhang et al., 2019b). The O 1s spectra of UWF comprise the two major diffraction peaks with 531.7 and 532.1 eV in Fig. 3d. The O1s peak at 532.8 eV of HP-β-CD/Fe_3O_4@WF exhibited a relatively lower intensity compared to that of UWF at 532.2 eV, indicating the consumption of carboxylic groups on the wool fiber due to modification. The observed peaks at 530.1eV can be attributed to Fe–O bonds in the O 1s spectra for HP-β-CD/Fe_3O_4@WF and HP-β-CD/Fe_3O_4@WF, confirming the existence of Fe_3O_4 particles in the modified wool fabrics (Afsharipour et al., 2021; Wang et al., 2023b). The N1s peak of modified wool at 400 eV was assigned to −N-C=O, which became weaker than that of UWF (Fig. 3e), which can be due to the b hydrolysis of peptide bonds during processing. In Fig. 3f, the characteristics peak of Fe2p3/2 and Fe2p1/2 of Fe_3O_4 are observed at 711.4eV and 724.8 eV for HP-β-CD/Fe_3O_4@WF and HP-β-CD/Fe_3O_4/LA@WF, respectively, which is consistent with previous study (Afsharipour et al., 2021). Furthermore, the Fe2p3/2 peak exhibit a split into two distinct peaks centered around 711eV and 713eV, corresponding to the Fe^{3+} and Fe^{2+} in Fe_3O_4 (Guo et al., 2022; Wang et al., 2023b). The C/N ratio exhibited a distinct disparity among UWF, HP-β-CD/Fe_3O_4@WF, and HP-β-CD/Fe_3O_4/LA@WF, as demonstrated in Table 1. The C/N ratio of both modified wool fabrics increased to 8.51 and 8.17 respectively, from the initial value of 5.8 for UWF. This could be attributed to the formation of a covalent bond between HP-β-CD capped Fe_3O_4 and the wool fiber, resulting in an elevated carbon

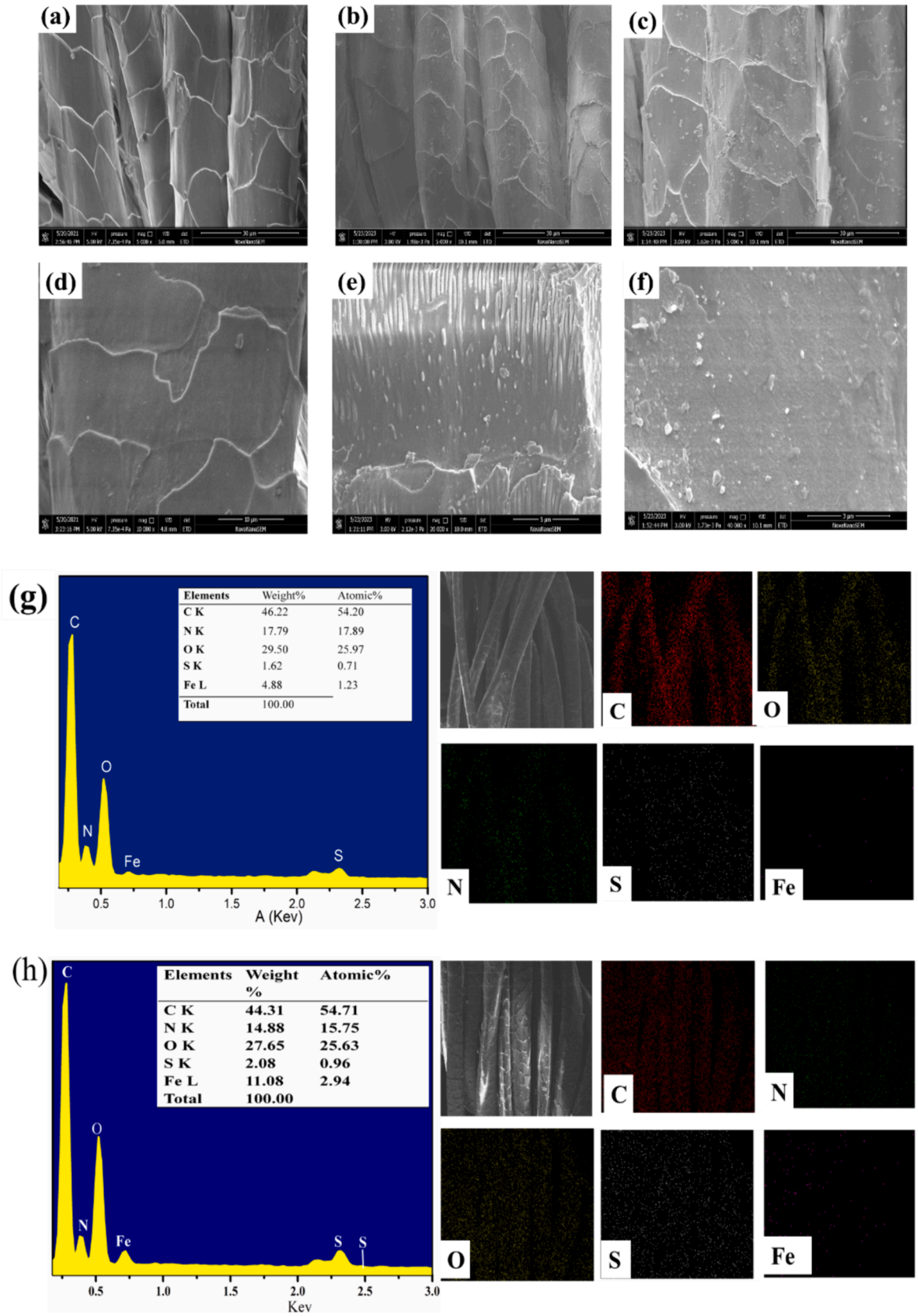

Fig. 2. Surface morphology and element analysis (a, d) untreated wool fabrics (b,e) HP-β-CD /Fe_3O_4@WF, (c,f) HP-β-CD /Fe_3O_4/LA0.2@WF; EDS of (g) HP-β-CD /Fe_3O_4@WF and (h) HP-β-CD /Fe_3O_4/LA@WF.

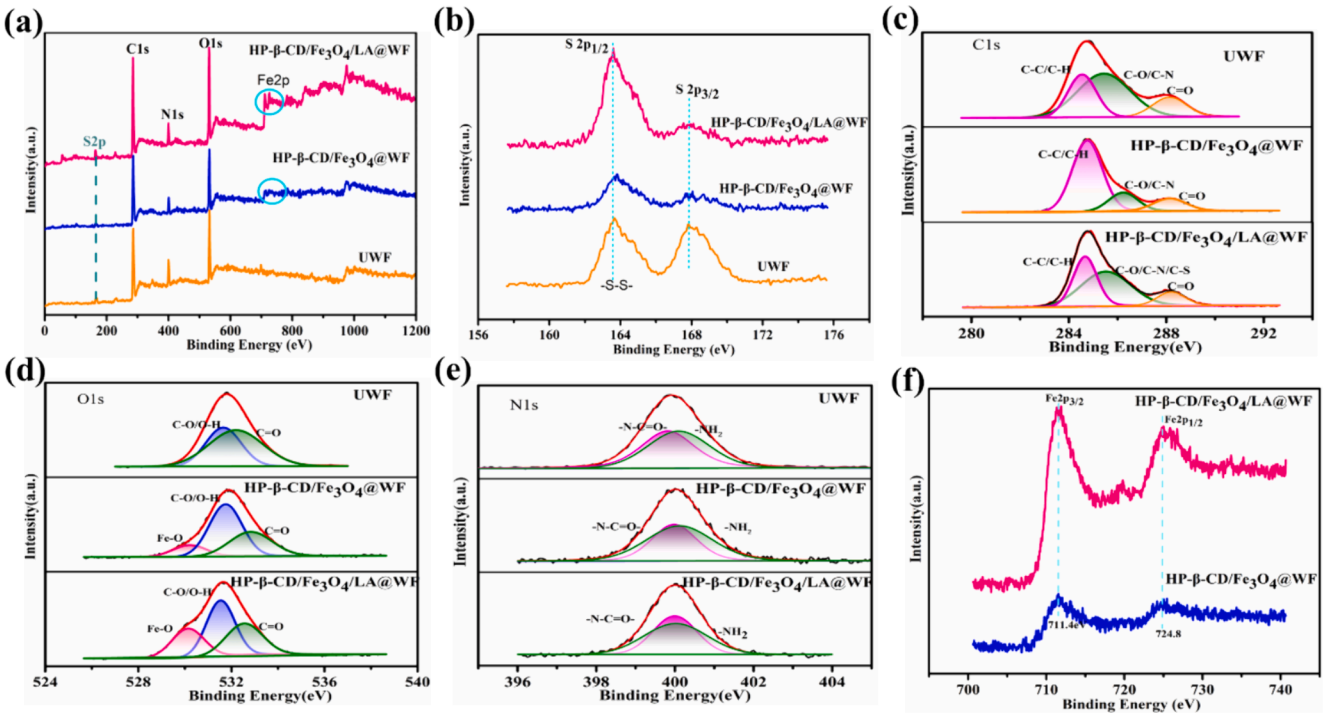

Fig. 3. (a)Survey XPS spectra, (b) S2p, (c) C1s, (d) O1s spectra, (e)N1s spectra, (f) Fe2p of wool fabrics with different treatments.

Table 1
Content of the Elements (Atom%) Obtained by XPS.

Samples	Content of the Elements(atom%)					Atomic ratio		
	C1s	**N1s**	**O1s**	**S2p**	**Fe2p**	**C/N**	**O/N**	**S/N**
UWF	64.98	11.21	20.59	3.22	–	5.80	1.84	0.29
HP-β-CD /Fe_3O_4@WF	67.78	7.96	20.13	2.1	2.03	8.51	2.53	0.26
HP-β-CD/Fe_3O_4/LA@WF	61.93	7.58	23.34	3.12	4.03	8.17	3.08	0.41

content. In the HP-β-CD/Fe_3O_4 modified process, the wool scales were wrapped by HP-β-CD, leading to an increase in carbon and oxidation elements. As a result, the C/N and O/N ratios of the modified wool samples exhibited higher values compared to untreated wool. In addition, compared with that of UWF and HP-β-CD/Fe_3O_4@WF, the higher S/N ratios of HP-β-CD/Fe_3O_4/LA@WF were also investigated due to the S-containing dithiolane of LA (Zhang et al., 2019b). These results demonstrated that the deposition of LA-coupled nanoparticles on the wool fibers.

3.2. *Properties of modified wool with LA dosage*

The color characteristics of modified wool fabrics with LA dosage before dyeing were comprehensively evaluated. Table 2 presents the lightness (L*), red or greenness (a*), blue or yellowness (b*), chroma or color saturation (c*) values, and samples images for untreated wool fabrics (UWF) and modified wool fabrics (MWF). The color of modified wool fabrics ranged from light-yellow to brown-yellow, depending on the LA dosages applied. This color change can serve as a reliable indicator for confirming the deposition of HP-β-CD capped Fe_3O_4 on the surface of wool. As shown in Table 2, the untreated wool fabrics exhibited L*, a*, and b* values of 79.57, 0.27 and 14.5, respectively. However, when using HP-β-CD/Fe_3O_4 on modified wool fibers, there was a significant decrease in L* (lightness) accompanied by an increase in both a*(redness) and b*(yellowness) values. The alteration in appearance can be attributed to the deposition of yellow–brown magnetic nanoparticles. With the increase of LA dosage, the hue of the modified wool fabrics gradually darkened into a yellowish-brown shade

Table 2
Color parameters of wool fabrics with different treatment.

Samples	L*	a*	b*	C*	Photographic images
UWF	79.6 ± 3.98	0.27 ± 0.014	14.5 ± 0.73	14.5 ± 0.73	
MWF-LA_0	72.6 ± 3.63	4.06 ± 0.20	24.02 ± 1.20	24.36 ± 1.22	
MWF-$LA_{0.1}$	67.2 ± 3.36	8.94 ± 0.45	30.4 ± 1.52	31.6 ± 1.58	
MWF-$LA_{0.2}$	66.3 ± 3.32	9.4 ± 0.47	29.6 ± 1.48	31 ± 1.55	
MWF-$LA_{0.3}$	66.8 ± 3.34	8.58 ± 0.43	27.6 ± 1.38	28.9 ± 1.45	
MWF-$LA_{0.4}$	68.6 ± 3.43	7.62 ± 0.38	26.8 ± 1.34	27.9 ± 1.39	

due to its inherent color from lipoic acid. Notably, MWF-LA_0 showed a b* value of 24 while MWF-$LA_{0.1}$ exhibited a significantly higher b* value of 30.4. This observed elevation in b* value with increasing LA dosage provides further evidence of a cross-linking reaction between LA and the amino acids derived from wool keratin (Zhang et al., 2019b). However, the hue became lighter beyond a dosage of 0.3g of LA due to the occurrence of ring-opening polymerization (Park & Lee, 2013).

The variations in properties of wool fabrics with different levels of LA dosages are illustrated in Fig. 4. As depicted in Fig. 4a, the untreated wool fabric exhibits the highest reflectance rate (R %), while after modification, the R % of wool fabric decreases with an increase in LA dosage. The presence of yellow–brown magnetic nanoparticles Fe_3O_4 and yellow lipoic acid contributes to their light absorption capacity. In Fig. 4b, the wrinkle recovery angle (WRA) of the modified wool surpasses that of the untreated wool fabrics and exhibits an increasing trend with higher LA dosage. When the LA dosage is increased to 0.3g, the WRA significantly rises from 156° of UWF to 215°. This increase can be attributed to the disulfide bond ring-opening polymerizations of lipoic acid occurring in the amorphous region of wool fibers, effectively filling the interspace between adjacent fibers and thereby enhancing fiber elasticity (Huang et al., 2021; Park & Lee, 2013). Wool exhibits a pronounced hydrophobicity primarily attributed to the presence of surface scales and a lipid layer structure (Hassan & Brorens, 2023; Parveen et al., 2021; Zhang et al., 2022a). The contact angle (CA) of untreated wool fabric (UWF) was measured at 126°, whereas HP-β-CD/Fe_3O_4@WF exhibited a reduced contact angle of 92° due to the presence of numerous hydrophilic (–OH) groups derived from hydroxypropyl-β-cyclodextrin (Zhang et al., 2019b). However, the surface contact angle of the modified wool increased with an increase in LA dosage, which can be attributed to the presence of hydrophobic disulfide bonds within lipoic acid (Mahlicli & Altinkaya, 2014).

The tensile strength of both modified wool fabrics exhibited a general decline compared to the untreated wool fabric, as depicted in Fig. 4c. The decrease in strength for HP-β-CD/Fe_3O_4@WF can be attributed to the deposition of HP-β-CD caped Fe_3O_4 on wool fiber, breaking the hydrogen bond between the peptide chain of wool. However, the strength, particularly the elongation at break, increases with the addition of lipoic acid. This can be attributed to the crosslinking effect of LA and the formation of a Poly-α-lipoic acid (PALA) film between wool fibers during hot pressing, which enhances the elasticity of wool fibers (Hosseinkhani et al., 2017).

3.3. UV protection, antioxidation and antibacterial properties

It is known that continuous exposure to UV radiations may lead to sunburn, premature aging, and potentially contribute to the occurrence of skin cancers. UV protection ability of modified wool fabrics was evaluated in terms of UPF (UV protection factor) in Fig. 4d. Compared to untreated wool fabrics, the UV resistance of modified fabrics is

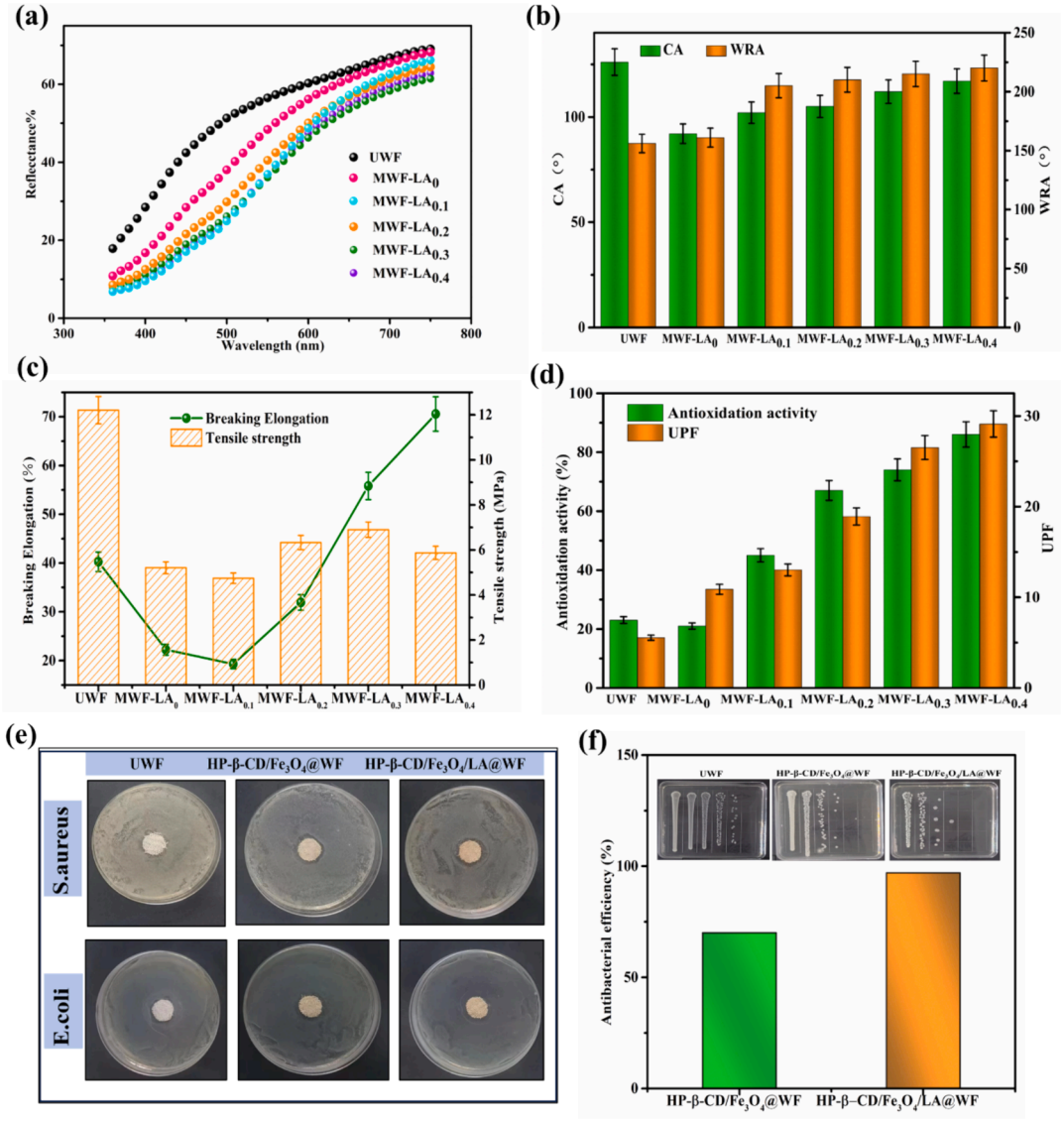

Fig. 4. (a) Reflectance rate; (b) Contact angle and wrinkle recovery angle; (c) Tensile strength and Elongation at break; (d) Antioxidation activity and UPF of different modified wool fabrics; (e) Antibacterial activity photograph;(f) Antibacterial efficiency.

enhanced. It was because that Fe_3O_4 nanoparticles are deposited onto the surface of wool fabrics, effectively adsorption on UV radiation (Shabbir et al., 2018). In addition, the formation of poly-α-lipoic acid film containing C=S, C=O, C=C groups on wool fiber also can absorb ultraviolet light, enhancing the UV resistance effect. Hence, with the LA dosage increase, UPF of modified wool fabric showed an upward trend.

The DPPH radical scavenging activities of various treated wool fabrics were quantified, and the results are depicted in Fig. 4d. It is evident that the UWF exhibited poor antioxidation activity; however, after modification, there was a noticeable increase in DPPH radical scavenging activities. Moreover, the antioxidant efficiency of modified wool fabrics showed an ascending tendency with the increase of the LA dosage. When using 0.4 g LA, the antioxidant activity reached 86%. The results were related to the good antioxidation activity of LA (Shi et al., 2016). The presence of more LA on the fabric facilitated in scavenging of the DPPH radicals and showed better antioxidant activity (Shen et al., 2020; Tan et al., 2022; Zhang et al., 2022a). The literature has reported the antibacterial efficacy of Fe_3O_4 against both gram-positive and gram-negative bacteria while lipoic acid has also demonstrated moderate antimicrobial activity (Prabhu et al., 2015; Shi et al., 2016; Yildiz et al., 2020). Hence, Lipoic acid coupled wool may cause cell membrane dysfunction of bacteria and the inhibition of DNA replication (Luo et al., 2020; Zhang et al., 2019b). The inhibitory effects on the growth of gram-positive Staphylococcus aureus (S. aureus) and gram-negative Escherichia coli (E. coli) were assessed using the inhibition zone test to evaluate their antibacterial properties. As shown in Fig. 4e, no inhibitory zone was observed on the agar plates when testing UWF against S. aureus and E. coli, indicating the absence of any antimicrobial properties exhibited by UWF against either of these bacteria. In contrast, HP-β-CD/Fe_3O_4@WF and HP-β-CD/Fe_3O_4/LA@WF exhibited effective antibacterial activities against S. aureus while showing ineffectiveness against E. coli. Furthermore, the bacteriostatic efficacy of modified wool fabrics was assessed using the shake flask testing method. HP-β-CD/Fe_3O_4/$LA_{0.3}$@WF was chosen as an example due to its superior absorption performance mentioned earlier, and the corresponding results are illustrated in Fig. 4f. The bacteriostatic rates of HP-β-CD/Fe_3O_4 @WF and HP-β-CD/Fe_3O_4/LA @WF were 70% and 97% against S. aureus, respectively. The antibacterial properties are generally attributed to the uniform deposition of positively charged Fe_3O_4 NPs onto the fiber surfaces. The efficacy of Fe_3O_4 NPs in eradicating bacteria can be attributed to their ability to generate reactive oxygen species (ROS), which effectively disrupt the outer bilayer of bacterial cells (Yildiz et al., 2020). Additionally, it is plausible that the electromagnetic attraction between positively charged Fe_3O_4 NPs and negatively charged microbes contributes to microbial oxidation and instantaneous death (Prabhu et al., 2015; Yildiz et al., 2020). After addition of LA, LA has been proved to exert its antimicrobial action through causing cell membrane dysfunction and changes in cellular morphology (Shi et al., 2016). Furthermore, LA was used as a couple agent to fix the HP-β-CD capped Fe_3O_4 nanoparticles to wool fiber, thus, thiolation of HP-β-CD/Fe_3O_4 increases the number of active groups on wool, thereby reinforcing the antibacterial property of HP-β-CD/Fe_3O_4/LA@WF. Overall, the modified wool fabric demonstrates the enhanced antibacterial properties.

3.4. Effect of different parameters on dyeing properties

3.4.1. LA dosage

Dyeing properties of the modified wool with various LA dosages were investigated under 4% (o.w.f) dye concentration, dyeing temperature of 60℃ for 60min without any pH adjustment. The results in terms of K/S value are presented in Fig. 5. The K/S value of dyed UWF with Curcumin and Acid red 1 is 0.63 and 1.08, respectively. After modification, the K/S values of wool fabrics significantly increased with the increase of LA dosage. As shown in Fig. 5a, the K/S values of dyed MWF with Curcumin steadily increased from 6.53 to 13.6 when LA dosage change from 0.1g to 0.4g, and the K/S increase was 51.99%. The K/S values of dyed MWF with Acid red 1 showed an upward trend with the LA dosage increase and the highest K/S value (23.5) can be obtained at 0.3g of LA in Fig. 5b. The enhanced dyeability of modified wool can be attributed to the presence of HP-β-CD capped Fe_3O_4 NPs with large specific surface area, which facilitate the adsorption of dye small molecular. In addition, the formation and deposition of poly-α-lipoic acid under hot-press introduces free carboxyl and hydroxyl on wool surface. These functional groups facilitate stronger interactions between dyes and wool fiber through ionic forces, hydrogen bonding, and van der Waals forces, resulting in outstanding color effect (Räisänen et al., 2023; Zhang et al., 2019b). However, further increasing the dosage of LA to 0.4 g did not significantly enhance the K/S values due to excessive polymerization of LA on the fiber surface, which hindered dye diffusion into the fiber interior. Therefore, a concentration of 0.3 g of LA was selected as the optimal treatment for wool and used in subsequent trial.

3.4.2. Dye bath pH

The pH level of the dye solution plays a crucial role in altering the distribution of charges on the wool surface, thereby affecting the dye adsorption process. The various pH was adjusted by Britton-Robinson buffer solution with 0.04 mol/L phosphoric acid, 0.04 mol/L boric acid, and 0.04 mol/L acetic acid to 1.87, 2.46, 3.57, 4.34, 5.17, 6.54 (Ebihara et al., 2016). The dyeing experiment was carried out with a dye concentration of 4% for dyeing 60min at 60℃. It is known that an acidic environment favors the dye uptake due to the protonation of amino groups on wool molecular structure (Räisänen et al., 2023). Therefore, the pH range was limited in an acid environment. The K/S values of dyed UWF and MWF with both dyes exhibited a gradual decrease as the initial pH value transitions from an acidic environment to a neutral one, as demonstrated in Fig. 6a and Fig. 6b. The corresponding images of dyed samples are exhibited in Fig. 6c and Fig. 6d. Notably, the highest K/S values were achieved at approximately pH 2.5 for both dyes. When the pH value was raised from 1.87 to 6.54, the K/S value of dyed MWF with Curcumin decreased from 17.4 to 4.5, while that with Acid red 1

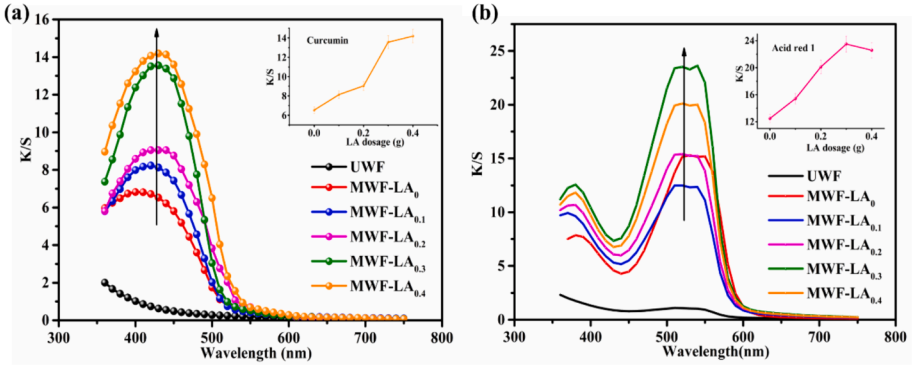

Fig. 5. K/S value of modified wool under different LA dosage: (a) Curcumin; (b) Acid red 1.

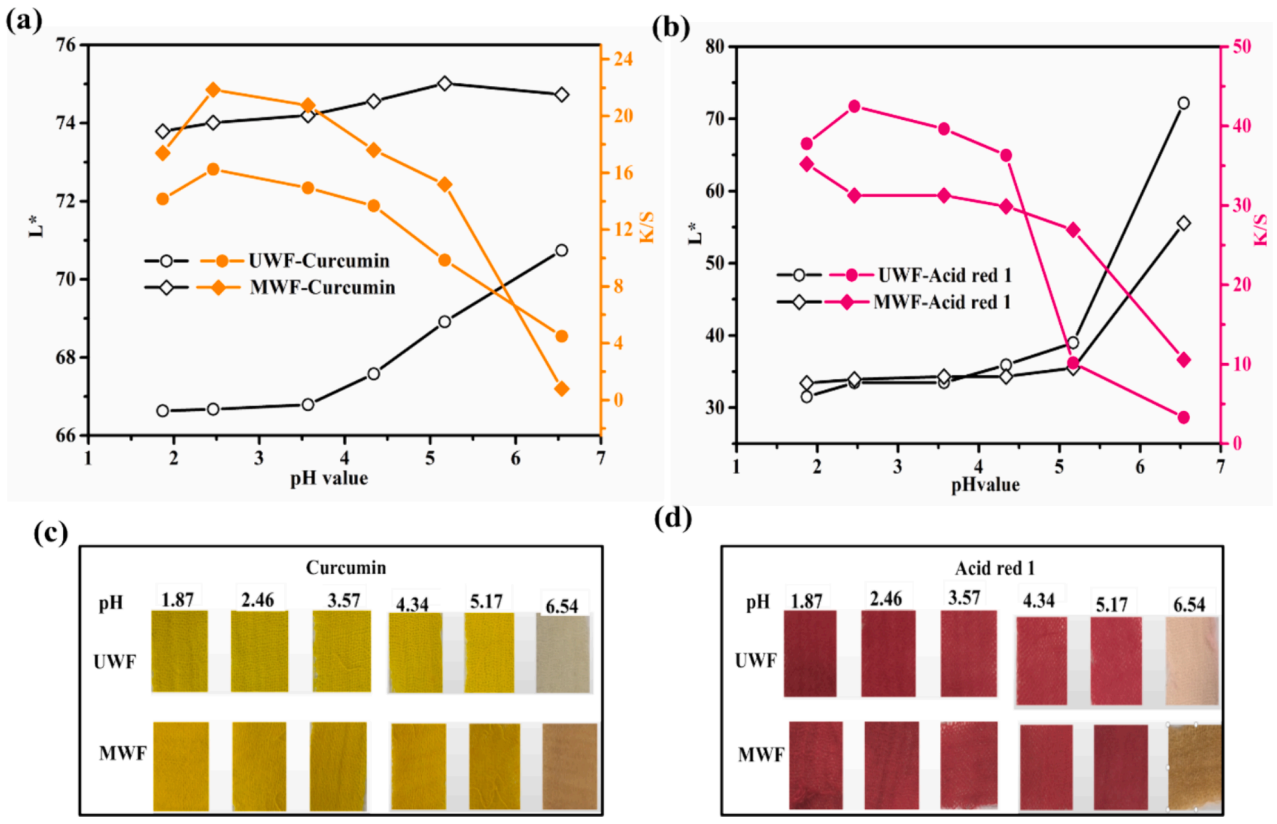

Fig. 6. Effect of pH value on L* and K/S of dyed wool fabrics: (a) and (c) Curcumin; (b) and (d) Acid red 1.

reduced from 35.2 to 10.6. Correspondingly, the L* value has a reverse change trend. The reason was that more amino group on the surface of the fiber was protonated into $-NH_3^+$ under acid conditions, enhancing the adsorption on dye molecular. Conversely, under alkaline conditions these protonated amino groups are deprotonated under alkaline conditions, leading to more repulsion between electronegative groups of wool fiber and dye, therefore, the K/S decreased (Wang et al., 2023a). However, considering the characteristics of the two dyes, to avoid the influence of pH on the experiments, the subsequent experiments were conducted without any pH adjustment (Zhan et al., 2023).

3.4.3. *Dyeing temperature*

The impact of dyeing temperature on HP-β-CD/Fe_3O_4/$LA_{0.3}$ modified wool fabrics was investigated. Wool fabrics were subjected to dyeing with 4% (o.w.f) curcumin and acid red 1 at various temperatures ranging from 30°C to 90°C, without pH adjustment. The photograph, CIE Lab color codes and color strength (K/S) of the dyed samples are shown in Fig. 7. After being dyed with curcumin under different temperature, the modified wool exhibits a distinct deep yellow hue and a higher positive values of b*in Fig. 7a, as compared to the light-colored appearance of the untreated wool. For the untreated wool fabric (UWF), the K/S value increases gradually with rising temperature while the lightness (L*) value shows an opposite trend. However, after modification, the corresponding K/S values exhibit a significant upward trend as the temperature rapidly increases. The K/S value of modified wool fabric (MWF) increased from 11.5 at 30 °C to 17.1 at 80 °C, indicating an enhanced dye uptake on the wool surface (Zhou et al., 2022). The MWF also exhibited a lower L* value of 55.7 at 80 °C, compared to the L values of 75.4 for UWF. In Fig. 7b, the dyed wool with Acid red 1 exhibits a red color with high positive values of a*. Similarly, the L * (lightness) dyed wool with Acid red 1 decreased while the K/S increased with the increase in the dyeing temperature. The highest K/S value for the Acid red 1 was obtained at 22.5 at 80 °C in Fig. 7b. The K/S value of MWF reached the maximum of 23.4 at 80 °C from 13.4 of 30 °C. The

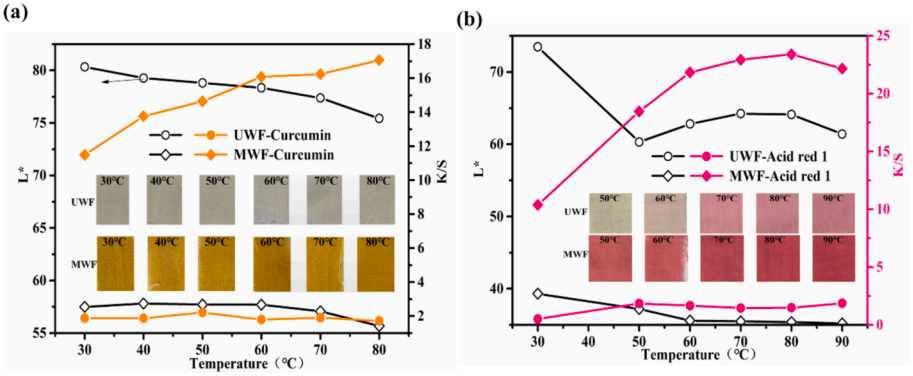

Fig. 7. Effect of dyeing temperature on L* and K/S of dyed wool fabrics: (a) Curcumin; (b) Acid red 1.

high temperature facilitates the opening of wool scales and enhances the penetration of dye into the inner structure of wool fibers (Xu et al., 2020b). The enhanced dyeability for MWF can be attributed to the introduction of more active groups and the presence of magnetic nanoparticles on the surface of wool fiber. Hence, the modified wool fabrics can achieve a deeper shade at the same dyeing temperature compared to the control wool dyeing, thereby significantly contributing to energy and water conservation (Räisänen et al., 2023; Sadeghi-Kiakhani et al., 2019). Based on the obtained results, the optimal dyeing temperature for modified wool fabrics was 80℃.

3.4.4. Dyeing time

The impact of time on the dyeing procss of UWF and MWF was investigated, and the corresponding images and results are presented in Fig. 8. Dyeing experiments were conducted using 4% Curcumin and Acid Red 1 at a temperature of 80℃ without pH adjustment. As shown in Fig. 8a and Fig. 8b, using curcumin dyeing, the surface color of UWF before 150min is very light, and the corresponding K/S is also very low, after that, the K/S significantly increases with time while the L* has the reverse tendency. Significantly different from this, the modified wool fabric showed rapid adsorption on curcumin within 15min of the first dyeing, the dyeing speed was very fast, and the K/S value was significantly increased. The K/S values of dyed UWF were 1.76, 6.4, and 11.3 at time intervals of 15 min, 150 min, and 240 min respectively. In contrast, the corresponding K/S values for dyed MWF were 19.3, 21.4, and 22.9, respectively at the same time. The results proved the diffusion rate of curcumin into the untreated fiber was slow at lower temperatures in the absence of an acidic environment, requiring a significantly longer duration for this process. The results of dyeing wool fabrics with Acid red 1 are presented in Fig. 8c and Fig. 8d. With the increase of time, the appearance color of UWF became darker, and K/S showed an increasing trend., Similarly, the change trend of L value is opposite to K/S. The K/S value of MWF obtained after dyeing for 15 min was found to be higher compared to that of UWF after dyeing for 240 min. The K/S value of the dyed UWF and MWF was 3.7 and 29.3 at 240 min, respectively. The K/S value of MWF was significantly higher than that of UWF for both dyes, which can be attributed to the presence of more functional groups on the modified wool surface, leading to enhanced interactions. Therefore, the results further proved that the HP-β-CD@Fe_3O_4/LA modification can impart highly efficient dyeing of wool fabrics.

3.4.5. Dye concentration

The dyeing properties of wool fabrics were investigated under various dye concentrations at a temperature of 80℃ for 150min. The dyeing images and results are shown in Fig. 9. With the increase of both dye concentration, the appearance color of the dyed UWF and MWF becomes darker in Fig. 9a and Fig. 9c. As shown in Fig. 9b and 9d, the K/S values of the modified samples exhibited a steady increase as the dye concentrations increased. Conversely, there was a decrease in the L* values with an increase in color strength. Using curcumin and Acid red 1 dyeing, the dyed MWF with 1% (o.w.f) dyes possessed higher K/S values than the dyed UWF with 8 % (o.w.f) dyes. For example, the K/S value of the dyed MWF with 1% (o.w.f) curcumin and Acid red 1 was 12.6 and 17.7, respectively, while the K/S of dyed UWF with 8 % (o.w.f) both dyes was 10.6 and 2.5, respectively. This emphasized that the modified wool can be dyed with the same color depth as conventional dyeing using a much lower amount of acid red 1 or curcumin. The remarkable enhancement in K/S of the modified wool fabrics can be attributed to the presence of HP-β-CD/Fe_3O_4/LA containing Fe-O, OH, and S-S on the wool surface, which enhanced the interactions between dyes and wool fiber through hydrogen bonding, and van der Waals forces, resulting in increased dye uptake and color strength (Sadeghi-Kiakhani et al., 2019).

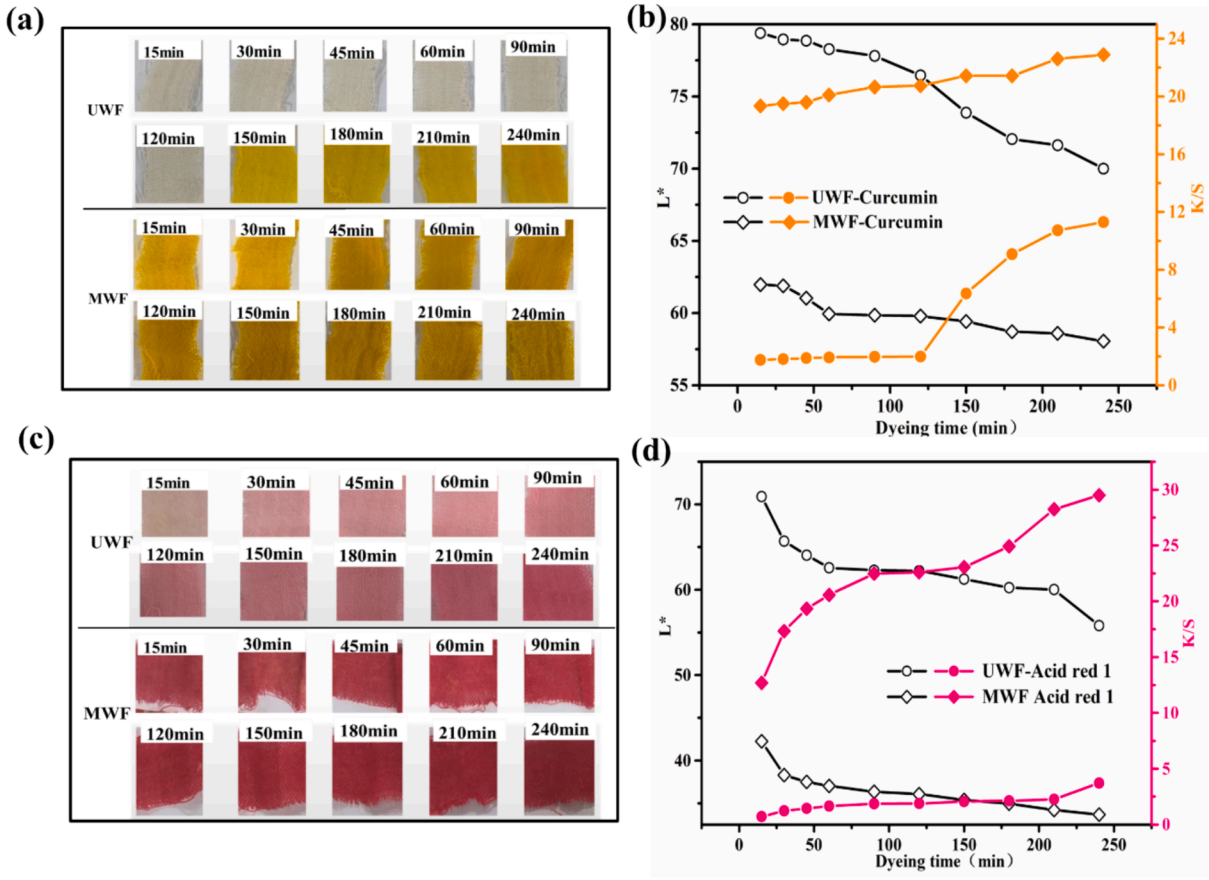

Fig. 8. Effect of dyeing time on L* and K/S of dyed wool fabrics: (a) and (b) Curcumin; (c) and (d) Acid red 1.

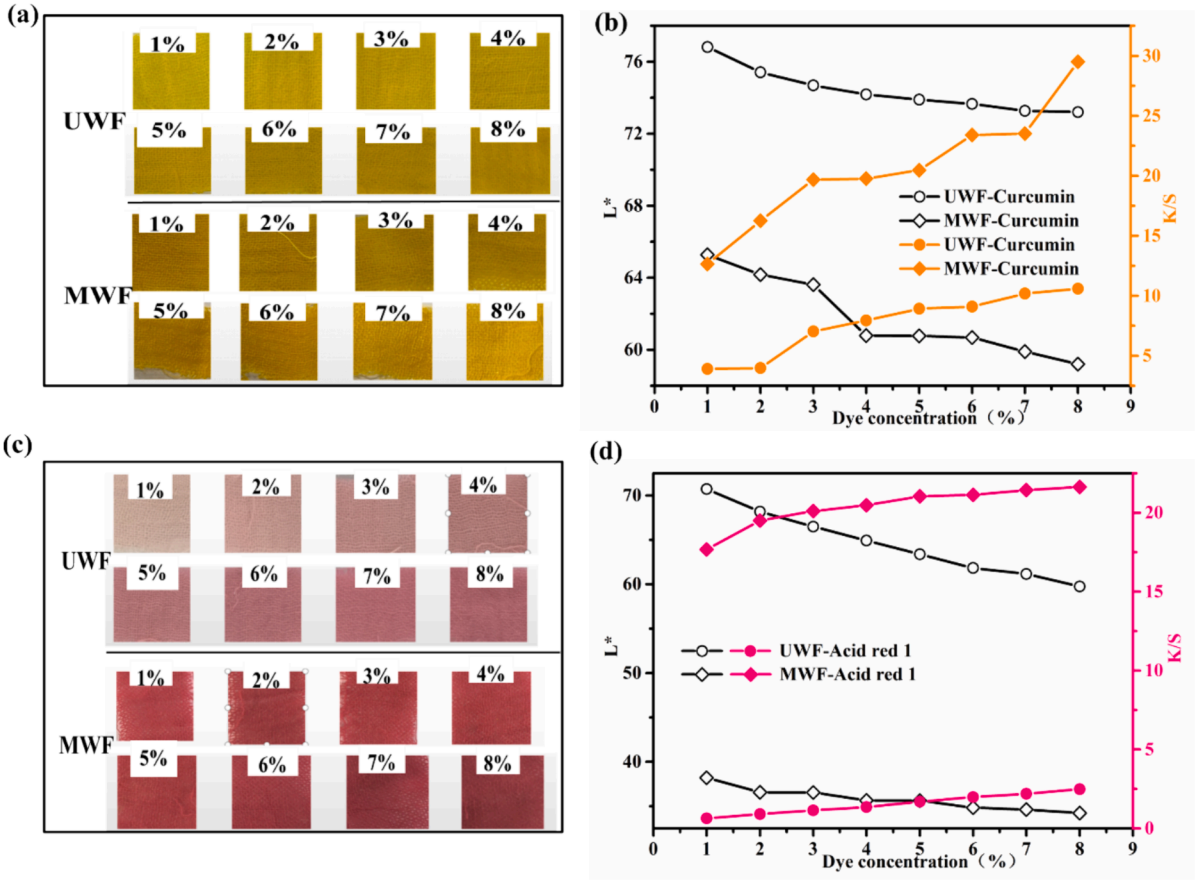

Fig. 9. Effect of dye concentration on L* and K/S of dyed wool fabrics: (a) and (b) Curcumin; (c) and (d) Acid red 1.

The results demonstrate that modification can effectively reduce the required amount of dye, enhance dyeing efficiency, and result in save cost savings.

3.5. *Color fastness of dyed wool fabrics*

The color fastness of untreated wool fiber (UWF) and modified wool fabric (MWF) was investigated after being dyed with 4% (o.w.f) Curcumin and Acid red 1, respectively, at 80℃ for 150min without pH adjustment. The washing, dry, and wet rubbing fastness rating of the dyed UWF and MWF samples were evaluated following the corresponding test method described in the experimental section (Rehman et al., 2021). The results are given in Fig. 10a and 10b. Compared to UWF, the dyed MWF obtained an improvement in coloration fastness. For example, using curcumin dyeing, the washing fastness of MWF reached 4 (excellent). The dry and wet rubbing of dyed MWF were excellent (4–5) and very good (4) respectively (Cai et al., 2023; Rehman et al., 2021; Zhang et al., 2019b). Using Acid red 1 dyeing, the washing and wet rubbing fastness of modified wool fabrics with HP-β-CD/Fe_3O_4/LA were improved to 4–5 grades in comparison to 3–4 grades of untreated fabric. The improved color fastness was attributed to the presence of more interaction between wool molecular chain and dyes, which came from the introduction of more active groups including S-S, hydroxyl, and carboxyl from HP-β-CD/Fe_3O_4/LA (Zhang et al., 2019b). The possible dyeing reaction mechanism is illustrated in Fig. 10c. These results further proved that the changes in surface properties of the modified wool with HP-β-CD/Fe_3O_4/LA play a crucial role in enhancing the interaction between dyes and fibers, as elaborated in previous sections.

4. Conclusions

In summary, an environmentally friendly modification method for enhancing the functionality and dyeability of wool fibers was established. The wool fibers were modified by utilizing HP-β-CD wrapped Fe_3O_4 nanoparticles and LA as couple agents. The results demonstrated the successful deposition of HP-β-CD capped Fe_3O_4 through LA coupling on the wool surface, enabling the functionalization of wool fabrics with tailored anti-crease properties, improved wettability, enhanced antioxidation and antibacterial activities, as well as enhanced dyeability properties. The HP-β-CD/Fe_3O_4/LA modified wool fabrics exhibited good antibacterial activity toward S. aureus with bacteriostatic rates of 97%. The dyed modified wool fabrics with curcumin and acid red 1 can attain higher color strength (K/S) than those of dyed untreated wool without additional agents. When using LA dosages of 0.3g, 4% (o.w.f) dye concentration, and dyeing temperatures of 80℃, the color strength of dyed MWF with Curcumin and Acid red 1 reached to 17.1 and 23.4 respectively without any pH adjustment. The washing, dry, and wet rubbing fastness rating of dyed HP-β-CD/Fe_3O_4/LA modified wool fabrics significantly improved. In all, the modification of HP-β-CD/Fe_3O_4/LA not only imparts wool fabric additional functionality but also enhances its dyeability, resulting in reduced dye dosage and cost savings, which facilitating clean dyeing processes and broadening their applications in the fields of medicine, healthcare, and technical textiles.

CRediT authorship contribution statement

Xuemei He: . **Guangyun Deng:** Visualization, Investigation, Data curation. **Zhengkang Zhang:** Software, Methodology. **Haiyan Mao:** Writing – review & editing, Project administration, Funding acquisition. **Lu Cai:** Writing – review & editing, Supervision, Formal analysis.

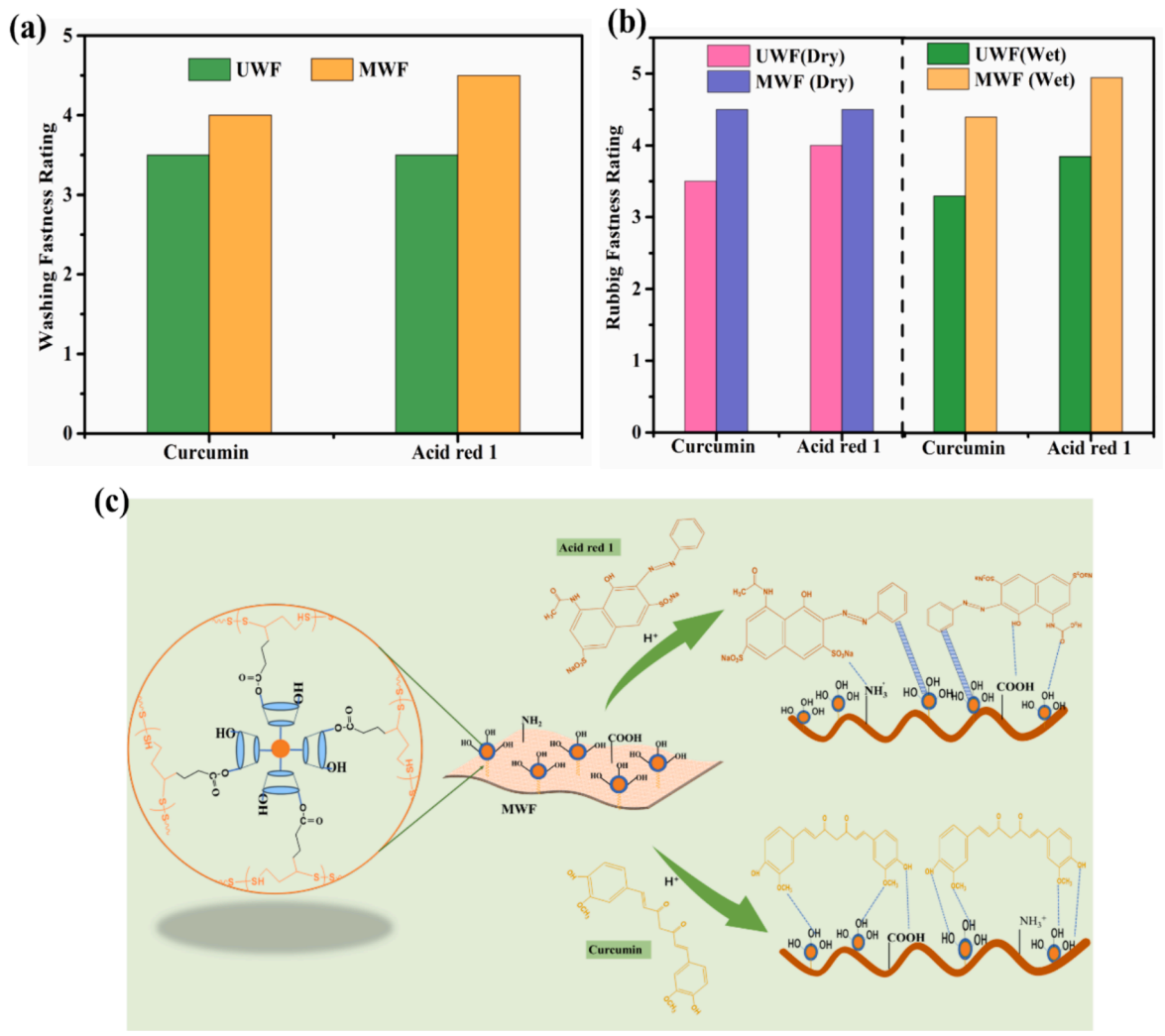

Fig. 10. Fastness properties and dyeing reaction mechanism of the dyed MWF: (a) Washing fastness; (b) Rubbing fastness; (c) Dyeing reaction mechanism.

Declaration of Competing Interest

The authors declare that they have no known competing financial interests or personal relationships that could have appeared to influence the work reported in this paper.

Acknowledgments

The authors gratefully acknowledge the financial support provided by the research fund of the National Natural Science Foundation of China (No: 52103067).

References

Adeel, S., Ahmad, S., Habib, N., Fazal ur, R., Mia, R., Ahmed, B., 2022. Coloring efficacy of Nyctanthes Arbortristis based yellow natural dye for surface-modified wool. Ind. Crop. Prod. 188, 115571.

Afsharipour, R., Dadfarnia, S., Shabani, A.M.H., Kazemi, E., Pedrini, A., Verucchi, R., 2021. Fabrication of a sensitive colorimetric nanosensor for determination of cysteine in human serum and urine samples based on magnetic-sulfur, nitrogen graphene quantum dots as a selective platform and Au nanoparticles. Talanta 226, 122055.

Aksu Demirezen, D., Demirezen Yılmaz, D., Yıldız, Y., 2023. Magnetic chitosan/calcium alginate double-network hydrogel beads: Preparation, adsorption of anionic and cationic surfactants, and reuse in the removal of methylene blue. Int J Biol Macromol 239, 124311.

Azab, D., Mowafi, S., El-Sayed, H., 2023. Simultaneous dyeing and finishing of wool and natural silk fabrics using Azolla pinnata extract. Emergent Materials 6 (4), 1329–1338.

Bahtiyari, M.İ., Yılmaz, F., 2018. Evaluation of Different Natural Dye Sources in Terms of Metamerism. AATCC J Res 5 (3), 21–27.

Banitorfi Hoveizavi, N., Feiz, M., 2023. Synthesis of novel dyes containing a dichlorotriazine group and their applications on nylon 6 and wool. Dyes Pigments 212, 111086.

Cai, Y., Xiao, L., Ehsan, M.N., Jiang, T., Pervez, M.N., Lin, L., Xiong, X., Naddeo, V., 2023. Green penetration dyeing of wool yarn with natural dye mixtures in D5 medium. J Mater Res Technol 25, 6524–6541.

Celebioglu, A., Uyar, T., 2019. Encapsulation and stabilization of α-lipoic acid in cyclodextrin inclusion complex electrospun nanofibers: Antioxidant and fast-dissolving α-lipoic acid/cyclodextrin nanofibrous webs. J. Agr. Food Chem. 67 (47), 13093–13107.

Çelik Yılmaz, N., Yılmaz, A., Yılmaz, F., 2023. Coloring of Woolen Fabrics with Natural Resources and Investigating the Color Perceptions of Children on These Fabrics. J Nat Fibers 20 (1), 2134269.

Corchete, P., Almagro, L., Gabaldon, J.A., Pedreno, M.A., Palazon, J., 2022. Phenylpropanoids in Silybum marianum cultures treated with cyclodextrins coated with magnetic nanoparticles. Appl Microbiol Biotechnol 106 (7), 2393–2401.

Dai, L., Yuan, J., Xu, J., Lou, J., Fan, X., 2023. Reversible bacteria-killing and bacteria-releasing cotton fabric with anti-bacteria adhesion ability for potential sustainable protective clothing applications. Int. J. Biol. Macromol. 253, 126580.

Dolinina, E.S., Akimsheva, E.Y., Parfenyuk, E.V., 2020. Development of novel silica-based formulation of α-lipoic acid: evaluation of photo and thermal stability of the encapsulated drug. Pharmaceutics 12 (3), 228.

Ebihara, A., Kawamoto, S., Shibata, N., Yamaguchi, T., Suzuki, F., Nakagawa, T., 2016. Development of a modified Britton-Robinson buffer with improved linearity in the alkaline pH region. J Biosci Bioeng 3, 2016.

El-Sayed, H., Mowafi, S., Basuoni, A.S., 2022. One-pot multi-functional finishing of wool fabric using reactive nonionic softener. Heliyon 8 (10), e10985.

Fazal ur, R., Adeel, S., Liaqat, S., Hussaan, M., Mia, R., Ahmed, B., Wafa, H. 2022. Environmental friendly bio-dyeing of silk using Alkanna tinctoria based Alkannin natural dye. Ind. Crop. Prod., 186, 115301.

Gu, J.Y., Dong, Y.C., Zhang, J.X., 2021. Comparative study of four different flavonoid compounds-containing plant extracts functionalised waste wool for accelerating aqueous chromium(VI) reductive removal. Color Technol 138 (1), 97–113.
Guo, S., Wang, H., Zhang, C., Li, L., Zhu, P., 2022. Efficient suppression of flammability in wool fabrics via chelation with ferric ions. Appl. Surf. Sci. 586, 152808.
Haque, A.N.M.A., Naebe, M., 2023. Zero-water discharge and rapid natural dyeing of wool by plasma-assisted spray-dyeing. J Clean Prod 402, 136807.
Hassan, M.M., Brorens, P., 2023. Strong insect-resist property and wash-durability exhibited by wool fabric sustainably treated with a natural diterpenoid and a synthetic pyrethroid under subcritical CO2. Colloid Surface A 671, 131595.
Hayat, T., Adeel, S., Fazal-ur-Rehman, Batool, F., Amin, N., Ahmad, T., Ozomay, M. 2022. Waste black tea leaves (Camelia sinensis) as a sustainable source of tannin natural colorant for bio-treated silk dyeing. Environ. Sci. Pollut. Res. Int., 29(16), 24035-24048.
He, X., Wu, C., Meng, C., Sun, L., Mao, H., Cai, L., 2022. Enhancement of natural dyeing properties and UV resistance of silk fibers modified by phenylboronic acid/hydroxypropyl-β-cyclodextrin functionalized Fe3O4 particle. J Appl Polym Sci 139 (27), e52253.
He, X., Zhu, T., Zhang, Z., Cai, L., Mao, H., 2024. An Effective Modification for Enhancing Bio-functionality and Coloration of Silk Fabrics with Chitosan/Alpha-Lipoic Acid Conjugates. Fiber. Polym. 25, 945–960.
Hosseinkhani, M., Montazer, M., Harifi, T., 2017. Protein and silver nitrate interaction during finer wool production: enhancing tensile properties along with synthesis of nano silver. J Text I 108 (1), 78–83.
Houshyar, S., Padhye, R., Shanks, R.A., Nayak, R., 2019. Nanodiamond Fabrication of Superhydrophilic Wool Fabrics. Langmuir 35 (22), 7105–7111.
Huang, C., Zhang, N., Wang, Q., Wang, P., Yu, Y., Zhou, M., 2021. Development of hydrophilic anti-crease finishing method for Cotton fabric using alpha-Lipoic acid without causing strength loss and formaldehyde release problem. Prog Org Coat 151, 106042.
Hwang, J.-S., An, J.-M., Cho, H., Lee, S.H., Park, J.-H., Han, I.-O., 2015. A dopamine-alpha-lipoic acid hybridization compound and its acetylated form inhibit LPS-mediated inflammation. Eur. J. Pharmacol. 746, 41–49.
Ikuta, N., Tanaka, A., Otsubo, A., Ogawa, N., Yamamoto, H., Mizukami, T., Arai, S., Okuno, M., Terao, K., Matsugo, S., 2014. Spectroscopic studies of R (+)-α-lipoic acid—cyclodextrin complexes. Int. J. Mol. Sci. 15 (11), 20469–20485.
Jiang, Z., Zhang, N., Wang, Q., Wang, P., Yu, Y., Yuan, J., 2021a. A controlled, highly effective and sustainable approach to the surface performance improvement of wool fibers. J. Mol. Liq. 322, 114952.
Jiang, Z., Zhang, Y.Y., Wang, Q., Wang, P., Yu, Y.Y., Zhou, M., Li, E.D., 2021b. Thiol-Based Ionic Liquid: An Efficient Approach for Improving Hydrophilic Performance of Wool. J Nat Fibers 19 (14), 9729–9740.
Li, B., Li, J., Shen, Y., Wu, H., Sun, Y., Zhang, P., Yang, M., 2022. Development of Environmentally Friendly Wool Shrink-Proof Finishing Technology Based on L-Cysteine/Protease Treatment Solution System. Int. J. Biol. Macromol. 23 (21), 13553.
Luo, Y., Cai, Z., Pei, L., Wang, J., 2023. Low temperature non-aqueous dyeing of wool fiber with reactive dyes: A sustainable and eco-friendly method. J. Clean. Prod. 432, 139803.
Luo, Q., Han, Q.Q., Chen, L.X., Fan, X.R., Wang, Y., Fei, Z.H., Zhang, H.M., Wang, Y.Q., 2020. Redox response, antibacterial and drug package capacities of chitosan-alpha-lipoic acid conjugates. Int. J. Biol. Macromol. 154, 1166–1174.
Mahlicli, F.Y., Altinkaya, S.A., 2014. Immobilization of alpha lipoic acid onto polysulfone membranes to suppress hemodialysis induced oxidative stress. J. Membr. Sci. 449, 27–37.
Maleki, G., Woltering, E.J., Mozafari, M.R., 2022. Applications of chitosan-based carrier as an encapsulating agent in food industry. Trends Food Sci. Tech. 120, 88–99.
Mia, M.S., Yao, P., Zhu, X.W., Lei, X., Xing, T.L., Chen, G.Q., 2021. Degradation of textile dyes from aqueous solution using tea-polyphenol/Fe loaded waste silk fabrics as Fenton-like catalysts. Rsc Advances 11 (14), 8290–8305.
Niu, Y., Wu, J., Kang, Y., Sun, P., Xiao, Z., Zhao, D., 2023. Recent advances of magnetic chitosan hydrogel: Preparation, properties and applications. Int. J. Biol. Macromol. 247, 125722.
Okasha, A.T., Abdel-Khalek, A.A., Alenazi, N.A., AlHammadi, A.A., Al Zoubi, W., Alhammadi, S., Ko, Y.G., Abukhadra, M.R., 2023. Progress of synthetic cyclodextrins-based materials as effective adsorbents of the common water pollutants: Comprehensive review. J Environ Chem Eng 11 (3), 109824.
Park, C.H., Lee, J., 2013. pH-dependent sustained release characteristics of disulfide polymers prepared by simple thermal polymerization. J. Biomat. Sci-Polym. e. 24 (16), 1848–1857.
Parveen, S., Rana, S., Goswami, P., 2021. Developing super-hydrophobic and abrasion-resistant wool fabrics using low-pressure hexafluoroethane plasma treatment. Materials (basel) 14 (12), 3228.
Prabhu, Y.T., Rao, K.V., Kumari, B.S., Kumar, V.S.S., Pavani, T., 2015. Synthesis of Fe3O4 nanoparticles and its antibacterial application. Int Nano Lett 5 (2), 85–92.
Racz, C.-P., Santa, S., Tomoaia-Cotisel, M., Borodi, G., Kacso, I., Pirnau, A., Bratu, I., 2013. Inclusion of α-lipoic acid in β-cyclodextrin. Physical–chemical and structural characterization. J. Incl. Phenom. Macro. 76 (1), 193–199.
Räisänen, R., Primetta, A., Toukola, P., Fager, S., Ylänen, J., 2023. Biocolourants from onion crop side streams and forest mushroom for regenerated cellulose fibres. Ind. Crop. Prod. 198, 116748.
Rama Rao, D., Gupta, V.B., 1992. Thermal characteristics of wool fibers. J Macromol Sci B 31 (2), 149–162.
Razmkhah, M., Montazer, M., Rezaie, A.B., Rad, M.M., 2021. Facile technique for wool coloration via locally forming of nano selenium photocatalyst imparting antibacterial and UV protection properties. J Ind Eng Chem 101, 153–164.
Rehan, M., Mashaly, H.M., Montaser, A.S., Abdelhameed, R.M., 2023. Decoration of wool fibers with mono or bimetallic nanoparticles for use in versatile applications. J. Mol. Liq. 387, 122603.
Rehman, A., Ahmad, A., Hameed, A., Kiran, S., Farooq, T., 2021. Green dyeing of modified cotton fabric with Acalypha wilkesiana leave extracts. Sustain. Chem. Pharm. 21, 100432.
Sadeghi-Kiakhani, M., Safapour, S., 2015. Functionalization of poly(amidoamine) dendrimer-based nano-architectures using a naphthalimide derivative and their fluorescent, dyeing and antimicrobial properties on wool fibers. Luminescence 31 (4), 1005–1012.
Sadeghi-Kiakhani, M., Safapour, S., Ghanbari-Adivi, F., 2019. Grafting of chitosan-acrylamide hybrid on the wool: Characterization, reactive dyeing, antioxidant and antibacterial studies. Int J Biol Macromol 134, 1170–1178.
Sadeghi-Kiakhani, M., Safapour, S., Habibzadeh, S.A., Tehrani-Bagha, A.R., 2021. Grafting of Wool with Alginate Biopolymer/Nano Ag as a Clean Antimicrobial and Antioxidant Agent: Characterization and Natural Dyeing Studies. J Polym Enviro 29 (8), 2639–2649.
Sadeghi-Kiakhani, M., Safapour, S., Golpazir-Sorkheh, Y., 2022. Sustainable Antimicrobial and Antioxidant Finishing and Natural Dyeing Properties of Wool Yarn Treated with Chitosan-poly(amidoamine) Dendrimer Hybrid as a Biomordant. J Nat Fibers 19 (15), 9988–10000.
Safapour, S., Mazhar, M., Nikanfard, M., Liaghat, F., 2022. Recent advancements on the functionalized cyclodextrin-based adsorbents for dye removal from aqueous solutions. Int J Environ Sci Te 19, 5753–5790.
Safapour, S., Rather, L.J., Mir, S.S., Shahid, M., Assiri, M.A., 2024a. Diversifying color palette of Prangos ferulacea colorants on wool yarns: dual mordant approach for enhanced color, antioxidant, and UV protection properties. J Text I, 1–13.
Safapour, S., Toprak-Cavdur, T., Rather, L.J., Assiri, M.A., Shahid, M., 2024b. Enhancing the Sustainability and Hygiene in the Dyeing of Wool Yarns with Prangos ferulacea Aerial Parts Extract in Conjunction with Metal-Biomordant Combinations. Fiber. Polym. 25 (6), 2169–2183.
Shabbir, M., Rather, L.J., Mohammad, F., 2018. Economically viable UV-protective and antioxidant finishing of wool fabric dyed with Tagetes erecta flower extract: Valorization of marigold. Ind Crop Prod 119, 277–282.
Shavandi, A., Ali, M.A., 2019. Graft polymerization onto wool fibre for improved functionality. Prog. Org. Coat. 130, 182–199.
Shen, F., Zhong, H., Ge, W., Ren, J., Wang, X., 2020. Quercetin/chitosan-graft-alpha lipoic acid micelles: A versatile antioxidant water dispersion with high stability. Carbohydr. Polym. 234, 115927.
Shi, C., Sun, Y., Zhang, X., Zheng, Z., Yang, M., Ben, H., Song, K., Cao, Y., Chen, Y., Liu, X., Dong, R., Xia, X., 2016. Antimicrobial effect of lipoic acid against Cronobacter sakazakii. Food Control 59, 352–358.
Singh, A., Khan, M.D., Sheikh, J., 2023. In-situ synthesis of a novel acid dye based on phosphonitrilic chloride trimer to develop coloured and flame-retardant wool. Polym Degrad Stabil 211, 110312.
Tan, W., Zhang, J., Mi, Y., Li, Q., Guo, Z., 2022. Synthesis and characterization of α-lipoic acid grafted chitosan derivatives with antioxidant activity. React. Funct. Polym. 172, 105205.
Teli, M.D., Pandit, P., 2017. Novel Method of Ecofriendly Single Bath Dyeing and Functional Finishing of Wool Protein with Coconut Shell Extract Biomolecules. ACS Sustain. Chem. Eng. 5 (9), 8323–8333.
Teli, M.D., Pandit, P., 2018. Application of Sterculia Foetida Fruit Shell Waste Biomolecules on Silk for Aesthetic and Wellness Properties. Fiber. Polym. 19 (1), 41–54.
Theodosis-Nobelos, P., Papagiouvannis, G., Tziona, P., Rekka, E.A., 2021. Lipoic acid. Kinetics and pluripotent biological properties and derivatives. Mol Biol Rep 48 (9), 6539–6550.
Wagner, A.F., Walton, E., Boxer, G.E., Pruss, M.P., Holly, F.W., Folkers, K., 1956. Properties and derivatives of α-lipoic acid. JACS 78 (19), 5079–5081.
Wang, M., Yi, N., Fang, K., Zhao, Z., Xie, R., Chen, W., 2023a. Deep colorful antibacterial wool fabrics by high-efficiency pad dyeing with insoluble curcumin. Chem. Eng. J. 452, 139121.
Wang, M., Zhao, H., Shi, F., Fang, K., Liang, Y., Xie, R., Chen, W., 2023b. Simple surface low temperature grafting for antibacterial and anti-felting inkjet printing wool fabrics. Prog. Org. Coat. 183, 107723.
Wang, H., Zhou, Y., Guo, Y., Liu, W., Dong, C., Wu, Y., Li, S., Shuang, S., 2012. β-Cyclodextrin/Fe3O4 hybrid magnetic nano-composite modified glassy carbon electrode for tryptophan sensing. Sensor Actuat B-Chem 163 (1), 171–178.
Ward, R.J., Willis, H.A., George, G.A., Guise, G.B., Denning, R.J., Evans, D.J., Short, R.D., 1993. Surface Analysis of Wool by X-Ray Photoelectron Spectroscopy and Static Secondary Ion Mass Spectrometry. Text Res J 63 (6), 362–368.
Wu, L.L., Bao, X.M., Ren, Y.W., Wang, P., Zhou, M., Yu, Y.Y., Wang, Q., 2022. Efficient regulation of dyeing behavior and physical properties of bombyx mori silks via graft polymerization of alpha-lipoic acid. Fiber. Polym. 23 (8), 2225–2233.
Xu, X.X., Gong, J.X., Li, Z., Li, Q.J., Zhang, J.F., Wang, L., Huang, J.F., 2020b. Mordant Free Dyeing and Functionalization of Wool Fabrics with Biocolorants Derived from Apocynum venetum L. Bast. *ACS Sustain. Chem. Eng.* 8 (33), 12686–12695.
Xu, L., Zhao, Z.X., Huang, Y.A., Zhu, Q.J., 2020a. Preparation of chitosan molecularly imprinted polymers and the recognition mechanism for adsorption of alpha-lipoic acid. Molecules 25 (2), 312.
Yan, B., Ren, Y., Ding, S., Zhou, M., Cui, L., Yu, Y., Wang, Q., Xu, B., Wang, P., 2022. A facile strategy for preparing silk fabrics with rapid photothermal antibacterial ability. Compos. Commun. 34, 101260.
Yildiz, A., Bayramol, D.V., Atav, R., Agirgan, A.O., Kurc, M.A., Ergunay, U., Mayer, C., Hadimani, R.L., 2020. Synthesis and characterization of Fe3O4@Cs@Ag

nanocomposite and its use in the production of magnetic and antibacterial nanofibrous membranes. Appl. Surf. Sci. 521, 146332.
Yilmaz, F., 2020. Application of Glycyrrhiza glabra L. Root as a Natural Antibacterial Agent in Finishing of Textile. *Ind Crop*. Prod 157, 112899.
Yılmaz, F., 2023. Application of Achillea millefolium as a Natural Antibacterial Agent in Finishing of Textile. Fiber. Polym. 24, 3175–3182.
Yılmaz, F., Aydınlıoğlu, Ö., Benli, H., Kahraman, G., Bahtiyari, M.İ., 2020. Treatment of originally coloured wools with garlic stem extracts and zinc chloride to ensure antibacterial properties with limited colour changes. Color Technol 136 (2), 147–152.
Yu, L., Xue, W., Cui, L., Xing, W., Cao, X., Li, H., 2014. Use of hydroxypropyl-β-cyclodextrin/polyethylene glycol 400, modified Fe3O4 nanoparticles for congo red removal. Int. J. Biol. Macromol. 64, 233–239.
Zare, A., 2023. Application of β-CD to Control the Release of ZnO Nanoparticles on the Silk Fabric Surface Along with Citric Acid as Eco-friendly Cross-linker. Progress in Color, Colorants and Coatings 16 (3), 295–307.
Zhan, J., Sun, H., Chen, L., Feng, X., Zhao, Y., 2023. Flexible fabrication chitosan-polyamidoamine aerogels by one-step method for efficient adsorption and separation of anionic dyes. Environ. Res. 234, 116583.
Zhang, N., Deng, Z., Wang, Q., Zhou, M., Wang, P., Yu, Y., 2022a. Phase-transited lysozyme with secondary reactivity for moisture-permeable antibacterial wool fabric. Chem. Eng. J. 432, 134198.
Zhang, X., Guo, Y., Li, W., Zhang, J., Wu, H., Mao, N., Zhang, H., 2021. Magnetically recyclable wool keratin modified magnetite powders for efficient removal of Cu(2+) ions from aqueous solutions. Nanomaterials (basel) 11 (5), 1068.
Zhang, N., Huang, P., Wang, P., Yu, Y., Zhou, M., Wang, Q., 2022b. Combined Cutinase and Keratinolytic Enzyme to Endow Improved Shrink-resistance to Wool Fabric. Fiber. Polym. 23 (4), 985–992.
Zhang, P., Wang, Q., Shen, J., Wang, P., Yuan, J., Fan, X., 2019a. Enzymatic Thiol-Ene Click Reaction: An Eco-Friendly Approach for MPEGMA-Grafted Modification of Wool Fibers. ACS Sustain. Chem. Eng. 7 (15), 13446–13455.
Zhang, P., Zhang, N., Wang, Q., Wang, P., Yuan, J., Shen, J., Fan, X., 2019b. Disulfide bond reconstruction: A novel approach for grafting of thiolated chitosan onto wool. Carbohydr. Polym. 203, 369–377.
Zhou, Q., Rather, L.J., Mir, S.S., Ali, A., Rizwanul Haque, Q.M., Li, Q., 2022. Bio colourants from the waste leaves of Ginkgo biloba L. tree: Wool dyeing and antimicrobial functionalization against some antibiotic-resistant bacterial strains. Sustain. Chem. Pharm. 25, 100585.
Zhu, J., Ma, N., Li, S., Zhang, L., Tong, X., Shao, Y., Shen, C., Wen, Y., Jian, M., Shao, Y., Zhang, J., 2023. Reinforced wool keratin fibers via dithiol chain Re-bonding. Adv. Funct. Mater. 33 (14), 2213644.